AD-A071 466 AERONAUTICAL RESEARCH LABS MELBOURNE (AUSTRALIA) F/G 1/1
LONGITUDINAL AERODYNAMICS EXTRACTED FROM FLIGHT TESTS USING A P--ETC(U)
OCT 78 R A FEIK

UNCLASSIFIED ARL/AERO NOTE-379 NL

| OF |
AD
A071466

END
DATE
FILMED
9-79
DDC

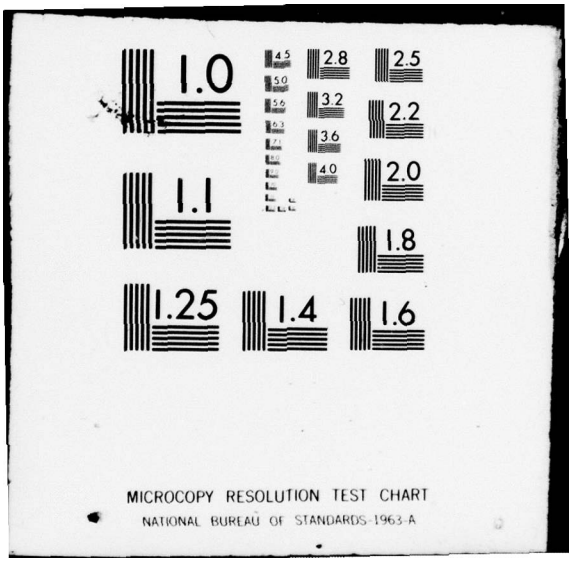
1.0
1.1
1.25
1.4
1.6
2.8
3.2
3.6
4.0
2.5
2.2
2.0
1.8
MICROCOPY RESOLUTION TEST CHART
NATIONAL BUREAU OF STANDARDS-1963-A

ARL-AERO-NOTE-379

AR-001-308

LEVEL

DEPARTMENT OF DEFENCE

DEFENCE SCIENCE AND TECHNOLOGY ORGANISATION

AERONAUTICAL RESEARCH LABORATORIES

MELBOURNE, VICTORIA

AERODYNAMICS NOTE 379

LONGITUDINAL AERODYNAMICS EXTRACTED FROM FLIGHT TESTS USING A PARAMETER ESTIMATION METHOD

by

R. A. FEIK

Approved for Public Release.

COPY No 12

OCTOBER 1978

AR-001-308

DEPARTMENT OF DEFENCE
DEFENCE SCIENCE AND TECHNOLOGY ORGANISATION
AERONAUTICAL RESEARCH LABORATORIES

(9) AERODYNAMICS NOTE 379

(6) LONGITUDINAL AERODYNAMICS EXTRACTED FROM FLIGHT TESTS USING A PARAMETER ESTIMATION METHOD.

by

(10) R. A. FEIK

(11) Oct 78

(12) 36 p.

SUMMARY

Flight data from a 60° delta wing aircraft have been analysed using a modified Newton–Raphson parameter estimation procedure. The model equations used for the analysis were extended to account for incidence vane errors and non-linearities in the pitching moment curves. Longitudinal derivatives extracted from the data have been compared with wind tunnel measurements and some theoretical estimates and areas of agreement and disagreement identified. The results demonstrate the usefulness of the parameter identification method not only for the validation of aircraft mathematical models and for checking flight results against wind tunnel data but also for obtaining aerodynamic data not easily available through other means.

(14) ARL/AERO Note-379

POSTAL ADDRESS: Chief Superintendent, Aeronautical Research Laboratories,
Box 4331, P.O., Melbourne, Victoria, 3001, Australia.

CONTENTS

1. INTRODUCTION

The use of systems identification techniques has been developing into a standard method for flight test analysis over the past few years. They provide for reduced flight testing time and more comprehensive data analysis[1] and have been applied to a variety of problems including high angle of attack "wing-rock" analysis[2] and determination of in-flight airload parameters[3] as well as the more common types of flight manoeuvre. From the point of view of mathematical modelling they provide a means for rational and systematic validation of a model and a means for obtaining additional data, which may not be available from wind tunnel tests, for use in such models.

A summary of various parameter estimation procedures applied to aircraft can be found in Reference 4, for example. One of these methods, the Modified Newton–Raphson technique as described in References 5 and 6, has been adapted for use on the ARL PDP10 computer. It was studied in some detail in Reference 7 with a view to using it in support of mathematical modelling activities. Briefly, referring to Figure 1, the method sets out to minimise a cost functional J, proportional to the difference between the measured response, $\mathbf{z}$, and the calculated response, $\mathbf{y}$,

$$J = (1/N)\sum_{i=1}^{N}(\mathbf{z}_i - \mathbf{y}_i)^T D_1(\mathbf{z}_i - \mathbf{y}_i) + (\mathbf{c} - \mathbf{c}_o)^T D_2(\mathbf{c} - \mathbf{c}_o) \tag{1}$$

where D_1 and D_2 are diagonal weighting matrices and the second term is a weighted mean square difference between the parameter vector, $\mathbf{c}$, and a stipulated *a priori* value, $\mathbf{c}_o$.

The mathematical model is described by the state equation

$$\dot{\mathbf{x}} = A\mathbf{x} + B\mathbf{u} \tag{2}$$

and the calculated response is

$$\mathbf{y} = F\mathbf{x} + G\mathbf{u} + \mathbf{b} \tag{3}$$

The measured response is assumed to be of the form

$$\mathbf{z} = \mathbf{y} + \mathbf{n} \tag{4}$$

where

$\mathbf{x}$ is the vector of state variables
$\mathbf{u}$ is the vector of control variables
$\mathbf{y}$ is the response vector
$\mathbf{b}$ is a measurement bias vector
$\mathbf{z}$ is the measured response vector
$\mathbf{n}$ is a random noise vector
A, B, F and G are matrices of parameters defining the model.

The parameter vector, $\mathbf{c}$, contains some or all of the elements of A, B, F and G, the elements of $\mathbf{b}$ and the initial conditions. The iterative Modified Newton–Raphson procedure is used to find the value of $\mathbf{c}$ which minimizes the cost, J. An indication of the quality of the estimates, $\mathbf{c}$, is given by the Cramer–Rao bound, σ_{CR}, which is a lower bound on the variance of the estimates.[6]

While Reference 7 considered more general aspects of the parameter estimation process including questions of response information requirements, control input design, data sampling rates, etc., this note describes the application of the Modified Newton–Raphson technique to the analysis of actual flight data in the form of aircraft longitudinal response to elevator input. The detailed model equations are outlined in Section 2. These include allowance for incidence vane errors on the one hand and extension of the model to treat aerodynamic non-linearities on the other. Section 3 describes the flight data including data conditioning prior to use in the analysis, and discusses the *a priori* values and weights used in the matching process. The results of the analysis and general discussion follow in Section 4 which also includes some comparison of the values of the extracted parameters with wind tunnel and/or theoretical values.

2. MATHEMATICAL MODEL

In this section the detailed form of the mathematical model described in general by Equations 2 and 3, is developed. Firstly, the basic linear small perturbation equations for aircraft longitudinal response are outlined. Next a simple extension of the equations is made in order to treat aerodynamic force and/or moment non-linearities within the context of a linear model. A further extension of the model then follows in order to deal with errors in the incidence vane measurements. Finally, one method for accommodating instrument lags and/or calibration errors is described.

2.1 Basic Model

It is assumed that the aircraft is trimmed in steady level flight with velocity V_e, incidence α_e and attitude θ_e. Small perturbation motions about this initial state are produced by elevator inputs. The linearised, uncoupled, longitudinal equations, written in body axes, to describe this motion, are (see for example Reference 8 for more details):

$$m\dot{u} = X_u u + X_\alpha \alpha + X_{\delta_e}\delta_e - mw_e q - mg\cos\theta_e\theta \tag{5a}$$

$$m\dot{w} = Z_u u + Z_\alpha \alpha + (Z_q + mu_e)q + Z_{\dot{\alpha}}\dot{\alpha} + Z_{\delta_e}\delta_e - mg\sin\theta_e\theta \tag{5b}$$

$$I_y\dot{q} = M_u u + M_\alpha \alpha + M_q q + M_{\dot{\alpha}}\dot{\alpha} + M_{\delta_e}\delta_e \tag{5c}$$

$$\dot{\theta} = q \tag{5d}$$

where $w_e = V_e \sin\alpha_e \simeq V_e\alpha_e$ and $u_e = V_e\cos\alpha_e \simeq V_e$ for small α_e.

For the short period mode it is further assumed that airspeed remains constant at the trim value, $V = V_e$. Then, from the definitions

$$(w + w_e) = V_e\sin(\alpha + \alpha_e) \text{ and } (u + u_e) = V_e\cos(\alpha + \alpha_e)$$

it follows that (for small α and α_e):

$$\dot{w} = V_e\dot{\alpha} \tag{6}$$

$$\text{and} \qquad u = -V_e(\alpha_e + 0{\cdot}5\alpha). \tag{7}$$

Thus Equation 5*b* for $\dot{w}$ becomes an equation for $\dot{\alpha}$ via Equation 6 while Equation 5*a* for $\dot{u}$ becomes redundant since u is related to α through Equation 7. Substituting for u from Equation 7 into Equations 5*b* and 5*c* leads to the short period approximations:

$$\begin{aligned}(mV_e - Z_{\dot{\alpha}})\dot{\alpha} &= [Z_\alpha - V_e(\alpha_e + 0{\cdot}5\alpha)Z_u]\alpha + (Z_q + mu_e)q + Z_{\delta_e}\delta_e - mg\sin\theta_e\theta \\ &\simeq Z_\alpha\alpha + mu_e q + Z_{\delta_e}\delta_e - mg\sin\theta_e\theta \end{aligned} \tag{8a}$$

$$\begin{aligned} I_y\dot{q} &= [M_\alpha - V_e(\alpha_e + 0{\cdot}5\alpha)M_u]\alpha + M_q q + M_{\dot{\alpha}}\dot{\alpha} + M_{\delta_e}\delta_e \\ &\simeq M_\alpha\alpha + M_q q + M_{\dot{\alpha}}\dot{\alpha} + M_{\delta_e}\delta_e \end{aligned} \tag{8b}$$

$$\dot{\theta} = q. \tag{8c}$$

These equations can be further simplified by noting that $Z_{\dot{\alpha}} \ll mV_e$. Substituting for $\dot{\alpha}$ in Equation 8*b* from Equation 8*a* gives

$$\begin{aligned} I_y\dot{q} &= (M_\alpha + M_{\dot{\alpha}}Z_\alpha/mV_e)\alpha + (M_q + M_{\dot{\alpha}}u_e/V_e)q + (M_{\delta_e} + M_{\dot{\alpha}}Z_{\delta_e}/mV_e)\delta_e - M_{\dot{\alpha}}g\sin\theta_e\theta/V_e \\ &\simeq M_\alpha\alpha + (M_q + M_{\dot{\alpha}})q + M_{\delta_e}\delta_e \end{aligned} \tag{8d}$$

where it has been assumed that $u_e \simeq V_e$ and the neglected terms are either much smaller than those retained or else make very little difference in the parameter estimation calculations. In each case the assumptions have been justified by the subsequent results.

An equation for the normal acceleration, n_z, follows from the definition

$$gn_z/V_e = (\dot{w} - u_e q + g\sin\theta_e\theta)/V_e \simeq (Z_\alpha/mV_e)\alpha + (Z_q/mV_e)q + (Z_{\delta_e}/mV_e)\delta_e. \tag{9}$$

Written in matrix notation the mathematical model used to analyse the short period motion can be summarized as follows. The state equations become:

$$\begin{bmatrix} \dot{\alpha} \\ \dot{q} \\ \theta \end{bmatrix} = \begin{bmatrix} Z_\alpha/mV_e & 1 & -g\sin\theta_e/V_e \\ M_\alpha/I_y & (M_q + M_{\dot{\alpha}})/I_y & 0 \\ 0 & 1 & 0 \end{bmatrix} \begin{bmatrix} \alpha \\ q \\ \theta \end{bmatrix} + \begin{bmatrix} Z_{\delta_e}/mV_e & Z_o \\ M_{\delta_e}/I_y & M_o \\ 0 & 0 \end{bmatrix} \begin{bmatrix} \delta_e \\ 1 \end{bmatrix}. \tag{10}$$

The equations for the response variables become:

$$\begin{bmatrix} \alpha \\ q \\ \theta \\ gn_z/V_e \end{bmatrix} = \begin{bmatrix} 1 & 0 & 0 \\ 0 & 1 & 0 \\ 0 & 0 & 1 \\ Z_\alpha/mV_e & Z_q/mV_e & 0 \end{bmatrix} \begin{bmatrix} \alpha \\ q \\ \theta \end{bmatrix} + \begin{bmatrix} 0 & 0 \\ 0 & 0 \\ 0 & 0 \\ Z_{\delta_e}/mV_e & Z_o \end{bmatrix} \begin{bmatrix} \delta_e \\ 1 \end{bmatrix} + \mathbf{b}. \tag{11}$$

The parameter vector is given by:

$$\mathbf{c} = [Z_\alpha/mV_e, Z_{\delta_e}/mV_e, M_\alpha/I_y, (M_q + M_{\dot{\alpha}})/I_y, M_{\delta_e}/I_y, Z_q/mV_e, Z_o, M_o]^T \tag{12}$$

where Z_o and M_o have been introduced to account for possible bias in the state and the measurement bias, **b**, appearing in Equation 11, has been left out of the parameter vector as it will be neglected from here on.

2.2 Model with Non-linear Aerodynamics

The basic model of Section 2.1 assumes linear aerodynamics. However it was obvious from inspection of the wind tunnel results of Reference 9 that at transonic speeds the pitching moment curve can be expected to be significantly non-linear with incidence, α. Over the present range of interest, i.e. $2° < \alpha + \alpha_e < 8°$, the wind tunnel curves suggest that the moment increment due to incidence needs to be modelled by a cubic equation, i.e.

$$\Delta M = M_\alpha\alpha + M_{\alpha^2}\alpha^2 + M_{\alpha^3}\alpha^3. \tag{13}$$

In order to accommodate this within the framework of a linear model, the α^2 and α^3 terms can be treated as known inputs with α^2 and α^3 becoming part of the input vector u together with δ_e. The time histories of α^2 and α^3 may be calculated directly from the measured values of incidence, α_m, or alternatively a purely linear model may be used initially with the resulting α time histories used to provide α^2 and α^3 for a subsequent matching in an iterative manner. As long as the non-linearities are relatively small this approach appears to be successful and the two alternatives for obtaining the histories of α^2 and α^3 produce only small differences in the final results.

The only equation altered by the inclusion of the "non-linear" terms is Equation 8*d* for pitch acceleration $\dot{q}$, which now becomes:

$$I_y\dot{q} = M_\alpha\alpha + (M_q + M_{\dot{\alpha}})q + M_{\delta_e}\delta_e + M_{\alpha^2}\alpha^2 + M_{\alpha^3}\alpha^3. \tag{14}$$

The matrix equations (Equations 10 and 11) are modified slightly with the control vector now becoming:

$$u = [\delta_e, \alpha^2, \alpha^3, 1]^T \tag{15}$$

and matrices B, G become 4×4 and 5×4 matrices respectively with the additional elements being zero with the exception of the two terms in B which correspond to M_{α^2}/I_y and M_{α^3}/I_y. Finally the parameter vector, **c** (Equation 12), is increased by the inclusion of M_{α^2}/I_y and M_{α^3}/I_y which need to be identified.

In some cases the Z-force also appears to be a non-linear function of incidence and a similar approach to the above may also be applied there. However, unless it is thought important to the model to include such additional parameters, the identification process may often be carried through quite successfully without them. That is to say, while the addition of such terms may make an improvement to the time history matches achieved, the estimated values of the other parameters of interest may differ very little. At the same time computational effort would increase.

2.3 Corrections to Incidence Vane Measurements

The incidence measurements are influenced by a pitch rate contribution, α_s, described as follows:

$$\alpha_m = \alpha - \alpha_s \tag{16}$$

where $$\alpha_s = (x_v/V_e)q$$

and x_v is the distance of the vane ahead of the centre of gravity.

Equation 16 can be modified to account for possible vane calibration slope errors as follows:

$$\alpha_m = G\,\alpha - \alpha_s \tag{17}$$

where G has to be estimated from the matching.

The vane was not dynamically balanced so that the strain gauges also responded to vane accelerations (see Reference 10 for more details). The correction to measured incidence due to normal acceleration at the vane can be written:

$$\alpha_d = K[\dot{q}(x_v/V_e) - gn_z/V_e] \tag{18}$$

where pitch acceleration, $\dot{q}$ is in radians/sec^2 and normal acceleration, n_z, is in g's, while the constant K depends on vane characteristics. The measured incidence, α_m, can now be related to the true incidence, α, by the equation:

$$\begin{aligned}\alpha_m &= G\alpha - \alpha_s - \alpha_d \qquad (19)\\ &= G\alpha - (x_v/V_e)q - K[\dot{q}(x_v/V_e) - gn_z/V_e]\end{aligned}$$

or
$$\alpha_m + \alpha_s = G\alpha - K[\dot{q}(x_v/V_e) - gn_z/V_e]. \tag{20}$$

By substituting for n_z and $\dot{q}$ from Equations 9 and 14, Equation 20 can be expanded to give:

$$\begin{aligned}\alpha_m + \alpha_s &= \{G - K[(x_v/V_e)\,M_\alpha/I_y - Z_\alpha/mV_e]\}\,\alpha - K[(x_v/V_e)\,(M_q + M_{\dot{\alpha}})/I_y - Z_q/mV_e]q -\\ &\quad - K[(x_v/V_e)\,M_{\delta_e}/I_y - Z_{\delta_e}/mV_e]\delta_e - K(x_v/V_e)\,(M_{\alpha^2}/I_y)\alpha^2 - K(x_v/V_e)\,(M_{\alpha^3}/I_y)\alpha^3\\ &= a_1\alpha + a_2 q + b_1\delta_e + b_2\alpha^2 + b_3\alpha^3. \qquad (21)\end{aligned}$$

The correction due to pitch rate, α_s, can be immediately calculated from Equation 16 since measurements of q are available. Thus $(\alpha_m + \alpha_s)$ rather than α_m is treated as a response variable which can be compared with the model results as calculated from the right hand side of Equation 21.

The full system of equations including non-linear pitching moment model and incidence vane corrections is summarized below.

The state equations are:

$$\begin{bmatrix}\dot{\alpha}\\ \dot{q}\\ \dot{\theta}\end{bmatrix} = \begin{bmatrix}Z_\alpha/mV_e & 1 & -g\sin\theta_e/V_e\\ M_\alpha/I_y & (M_q + M_{\dot{\alpha}})/I_y & 0\\ 0 & 1 & 0\end{bmatrix}\begin{bmatrix}\alpha\\ q\\ \theta\end{bmatrix} + \begin{bmatrix}Z_{\delta_e}/mV_e & 0 & 0 & Z_o\\ M_{\delta_e}/I_y & M_{\alpha^2}/I_y & M_{\alpha^3}/I_y & M_o\\ 0 & 0 & 0 & 0\end{bmatrix}\begin{bmatrix}\delta_e\\ \alpha^2\\ \alpha^3\\ 1\end{bmatrix} \tag{22}$$

The response equations are:

$$\begin{bmatrix}\alpha\\ q\\ \theta\\ \alpha_m + \alpha_s\\ gn_z/V_e\end{bmatrix} = \begin{bmatrix}1 & 0 & 0\\ 0 & 1 & 0\\ 0 & 0 & 1\\ a_1 & a_2 & 0\\ Z_\alpha/mV_e & Z_q/mV_e & 0\end{bmatrix}\begin{bmatrix}\alpha\\ q\\ \theta\end{bmatrix} + \begin{bmatrix}0 & 0 & 0 & 0\\ 0 & 0 & 0 & 0\\ 0 & 0 & 0 & 0\\ b_1 & b_2 & b_3 & b_o\\ Z_{\delta_e}/mV_e & 0 & 0 & Z_o\end{bmatrix}\begin{bmatrix}\delta_e\\ \alpha^2\\ \alpha^3\\ 1\end{bmatrix}. \tag{23}$$

The parameter vector now is:

$$\begin{aligned}\mathbf{c} = [&Z_\alpha/mV_e, Z_{\delta_e}/mV_e, M_\alpha/I_y, (M_q + M_{\dot{\alpha}})/I_y, M_{\delta_e}/I_y, M_{\alpha^2}/I_y,\\ &M_{\alpha^3}/I_y, Z_q/mV_e, a_1, a_2, b_1, b_2, b_3, Z_o, M_o, b_o]^T\end{aligned} \tag{24}$$

where b_o has been added to account for possible state bias. The measurement bias vector, **b**, has again been assumed to be zero. The coefficients a_1, a_2, b_1, b_2 and b_3 have been treated as unknown parameters to be estimated. Alternatively, an estimate for K can be made from the known inertial and aerodynamic characteristics of the vane and approximate values of these coefficients established. The less critical ones, such as b_2 and b_3 may be fixed and only a_1, a_2 and b_1 then allowed to vary. The subsequently identified values of a_2 and b_1 can then be used in the definitions of a_2 and b_1 (Equation 21) to obtain two values for K. Hopefully these values will be in reasonable agreement with each other and with the previously estimated value. Having obtained K in this way a value for G follows from a_1 (Equation 21).

2.4 Instrument Lags and Calibration Errors

Calibration errors and lags in instrumentation can be modelled in the state equations. For example, if a lag and/or calibration change is suspected in the incidence measurements, the following model could be postulated:

$$\frac{d\alpha_m}{dt} + \frac{\alpha_m}{\tau} = \frac{G\alpha}{\tau}. \tag{25}$$

Where τ is the lag time constant and G would account for any change in calibration slope. The values of τ and G would then be identified for optimum match. Such an approach was initially used to improve the match of the incidence record and although an improvement was achieved, as may be expected when two additional free parameters are provided, it was obvious from the results that this approach was inadequate and much better results were obtained using the corrections outlined in Equation 2.3. This will be more fully discussed in Section 4.

3. FLIGHT DATA

This section discusses the flight data to be analysed. The form of the data and the conditions under which they were obtained are first outlined followed by a description of corrections and pre-processing applied to the data in preparation for the Modified Newton–Raphson program. Finally, the *a priori* values used for each of the parameters are summarized followed by a discussion of the values chosen for the elements of the weighting matrices D_1 and D_2.

3.1 Test Conditions

The data available relate to flight tests performed on a 60° delta wing fighter aircraft. The manoeuvres considered in the present study are aircraft pitch response to pilot input in the form of an elevator pulse. Flights at two different Mach numbers were analysed, namely $M = 0{\cdot}96$ and $0{\cdot}71$. Other relevant conditions for these flights, referred to as flights 210 and 211 respectively, are summarized in Table 1.

TABLE 1
Flight Test Conditions

Details	Flight 210	Flight 211
M	0·96	0·71
h	9019 m (29 590 ft)	2971 m (9746 ft)
V_e	292·2 m/s (568 kt)	233·8 m/s (454 kt)
α_e	3·64°	2·64°
θ_e	3·28°	2·47°
$(\delta_e)_e$	−0·63°	−0·82°
c.g.	50·49% of ℄ chord	49·10% of ℄ chord
K	0·293	0·234

The values of K given in Table 1 were estimated from data given in Reference 10. From Equation 18 it follows that

$$Kg/V_e = \alpha_d/[\dot{q}(x_v/g) - n_z], \text{ rad/g}$$

Now for an effective vane mass of 0·325 kg, the inertial force per g = 3·18 N. On the other hand, from wind tunnel calibrations,[10] force per radian = 323·074 N so that equivalent radians per g for the inertial force = 3·18/323·074 = 0·00984 = Kg/V_e. Thus

$$K = 0{\cdot}00984\ V_e/g. \tag{26}$$

Measured data consisted of response time histories of α, q, n_z and δ_e. Approximately 15 seconds of record was available but only the 5 seconds following (and including) the pulse input was used in the analysis. This represented approximately 2 to 3 cycles of oscillation.

The data rate was 60 samples/second and from inspection of the flight records it was determined that the natural frequency ω_n for flight 210 was approximately 3·9 rad/s while for flight 211 it was approximately 4·5 rad/s. Using an in-between value of 4·2 rad/s it follows that

$$\begin{aligned} \omega_n \Delta t &= 4{\cdot}2/60 \quad = 0{\cdot}07 \\ \omega_n T &= 4{\cdot}2 \times 5 = 21 \end{aligned} \tag{27}$$

where Δt is the sampling interval and T is the total record length.

The values of $\omega_n \Delta t$ and $\omega_n T$ from Equation 27 compare with the values of $\omega_n \Delta t < 0{\cdot}14$ and $\omega_n T > 14$ found in Reference 7 to be adequate for matching of the Dutch Roll response to rudder doublet input. In both cases the systems are predominantly second order though the present case differs from that of Reference 7 in having a pulse rather than a doublet input. On the other hand the present system of equations is simpler with fewer parameters. It may be expected then that the sampling rate and record length requirements for successful identification would be similar and in fact no difficulties of convergence or identification were encountered in the present analysis. Less stringent values of $\omega_n \Delta t$ and $\omega_n T$ than those in Equation 27 would also be expected to lead to successful analysis. Although 10 iterations were normally specified in the program, good convergence was generally achieved by about 5 iterations or less with only small improvements subsequently.

3.2 Data Conditioning

Before proceeding with the analysis a certain amount of manipulation and/or correction of data was necessary. This included the following:

(*a*) Normal accelerometer corrections for location errors according to the equation (Reference 8):

$$n_{z_m} = n_z - (x_a\dot{q} - y_a\dot{p} + z_a q^2 + z_a p^2)/g \tag{28}$$

where n_{z_m} is the measured acceleration, n_z is the value at the centre of gravity and x_a, y_a, z_a are the co-ordinates of the accelerometer relative to the aircraft body axes. If measurements of angular accelerations, $\dot{p}$ and $\dot{q}$, are not available, the identification can proceed initially without this correction and if they are thought to be important the values calculated via the identified model used in a second iteration. In the present work, these corrections were generally small.

(*b*) Pitch rate gyro corrections for misalignment according to the equations given in Reference 8 (p. 31). Using the gyro alignment data the corrected pitch rate, q, is obtained from the measured roll, p_m, pitch, q_m, and yaw, r_m, rates according to the equation

$$q = 0{\cdot}0302\, p_m + 1{\cdot}00087\, q_m - 0{\cdot}0082\, r_m. \tag{29}$$

(*c*) Angle of incidence corrections for pitch rate effect as discussed in Section 2.3. The corrected incidence becomes $\alpha_m + \alpha_s$ where α_m is the measured value and α_s is given by Equation 16.

(*d*) A smooth curve was fitted by hand to the elevator input data as shown in Figures 2 and 3. The effect of this smoothing on the results was hardly discernible, especially for flight 210 where the measurement noise was small but for cases with higher noise levels on the measured input smoothing should minimize the standard deviations of the identified parameters and should be worthwhile provided inadvertent errors are not introduced in the process.

(e) Non-zero steady state values of elevator angle, $(\delta_e)_e$, incidence, α_e, and normal acceleration, n_{z_e} $(=1)$, were subtracted from the respective records so that the increments remaining could be compared directly with results of the small perturbation model.

3.3 *A Priori* Values and Weighting Matrices

The *a priori* values which were ascribed to the various parameters were mainly obtained from wind tunnel tests (e.g. Reference 9) or else were estimated from data sheet sources. Table 2 summarises the values used in the two cases analysed.

TABLE 2
***A Priori* Parameter Values**

Parameter	Flight 210	Flight 211
Z_α/mV_e	−0·848	−1·145
Z_{δ_e}/mV_e	−0·314	−0·467
M_α/I_y	−25·49	−19·78
$(M_q + M_{\dot\alpha})/I_y$	−1·02	−2·38
M_{δ_e}/I_y	−35·46	−31·14
M_{α^2}/I_y	0	—
M_{α^3}/I_y	0	—
Z_q/mV_e	0	0
a_1	0·93	0·87
a_2	0·0091	0·0134
b_1	0·24	0·231
b_2	−0·28	—
b_3	14·70	—
Z_o	0	0
M_o	0	0
b_o	0	0

The pitching moment derivatives have been adjusted to the correct centre of gravity position for each flight. The parameters relating specifically to the non-linearities of the pitching moment curve, namely M_{α^2}/I_y, M_{α^3}/I_y, b_2 and b_3 are absent for flight 211 since in that case the moment curve is reasonably linear over the incidence range of interest.

The *a priori* value of Z_q/mV_e has been set to zero since, for a delta wing it is expected to be small and is difficult to estimate. In later calculations Z_q/mV_e was neglected as it was found to have very little effect on the fit error or on the other estimated parameters. For a_1, a_2, b_1, b_2 and b_3 the *a priori* values were calculated by assuming $G = 1$ and $K = 0{\cdot}3$ in the formulae summarised by Equation 21. The parameters b_2 and b_3 were only used in later runs and previously identified values of M_{α^2} and M_{α^3} were used to calculate the *a priori* values shown in Table 2.

The elements of D_2 fix the weighting to be assigned to each of the *a priori* values. These were set by assuming a standard deviation, σ, equal to 20% of the parameter value. The relevant element of D_2 is then equal to $1/\sigma^2$. Very little difference in the identified results was obtained by assuming a 10% standard deviation but smaller values of σ tend to push the identified parameter values towards the *a priori* values, especially with the more weakly identified parameters. This effect, together with the relative magnitudes of the Cramer–Rao bound helps to isolate the weaker parameters (i.e. those that only weakly influence the results) if they are not already known. Referring to Table 2, those parameters with zero *a priori* value are ascribed a large standard deviation (99999 say) which leads to an effectively zero weighting element in D_2.

The elements of D_1 fix the weighting to be assigned to each of the time histories being matched, e.g. $\alpha_m + \alpha_s$, q and gn_z/V_e in the present case. No attempt was made to relate the elements of D_1 to the instrument accuracies but rather, in order to give approximately equal

weighting to each matched time history, a standard deviation, σ_m, equal to 5% of the maximum value of each measured record was selected and the relevant element of D_1, equal to $1/\sigma_m^2$, then calculated. The resulting weights are summarised in Table 3 below.

TABLE 3
Elements of Weighting Matrix D_1

Response Element	Flight 210	Flight 211
α	0·001	0·001
q	5328	6400
θ	0·001	0·001
$(\alpha_m + \alpha_s)$	91827	81633
gn_z/V_e	147929	49383

For records not being matched the corresponding element of D_1 was set to a small value. This applies to α and θ in Table 3. In the case of θ, no measurements were available for matching while in the case of α, the corrected value $\alpha_m + \alpha_s$ is being matched rather than α itself.

4. RESULTS

In this section the results of the identification are presented. Two particular aspects which arose during the matching process are first discussed in some detail. One involves the angle of incidence vane corrections, illustrated by reference to flight 211, while the other describes the influence of non-linearity in the pitching moment *vs.* incidence curve, prominent only in flight 210 at $M = 0{\cdot}96$. Following this, some general observations arising out of the results from both flights will be made.

4.1 Matching of Angle of Incidence Measurements

Table 4 summarises the results obtained from flight 211 and, as a reference, shows in the first column the *a priori* values and weights (based on 20% of *a priori* value) of the various parameters of interest.

The column headed 211–1 lists the results obtained when only the q_m and n_{z_m} records were matched using the basic mathematical model described in Section 2.1. The resulting fits to q_m and n_{z_m} were very good as shown by the small values of the mean square weighted errors $s^2(q)$ and $s^2(gn_z/V_e)$ obtained. The identified values of Z_α/mV_e, Z_{δ_e}/mV_e and M_{δ_e}/I_y differ only slightly from the *a priori* values, while M_α/I_y is approximately 11% down. The largest change, however is in the damping parameter $(M_q + M_{\dot\alpha})/I_y$ which is little more than half the *a priori* value.

Although for case 211–1 no attempt was made to match the α_m record it is, nevertheless, of interest to compare the mathematical model calculation of incidence, α, with the measured value, α_m. This is shown in Figure 4*a* and is obviously not very satisfactory. If, now, the uncorrected α_m record is included in the matching process, together with q_m and n_{z_m}, the results of column 211–2 apply and the match achieved, for angle of incidence is shown in Figure 4*b*. This is an improvement on the results of Figure 4*a* but is far from being good with a relatively large mean square error, $s^2(\alpha)$ of 2·78. In addition, the match achieved with the q_m and n_{z_m} records has deteriorated markedly compared to case 211–1 with $s^2(q)$ going from 0·18 to 1·14 and $s^2(gn_z/V_e)$ going from 0·078 to 0·14. The values of the identified derivatives also vary from that obtained in case 211–1. Most significantly, the attempt to reconcile the three traces α_m, q_m and n_{z_m} has led to quite large changes in the values of M_{δ_e}/I_y and $(M_q + M_{\dot\alpha})/I_y$.

TABLE 4
Results from Flight 211

Item	*A Priori*	211–1	211–2	211–3	211–4
Z_α/mV_e	$-1{\cdot}14\pm0{\cdot}23$	$-1{\cdot}10\pm0{\cdot}16$	$-1{\cdot}26\pm0{\cdot}16$	$-1{\cdot}12\pm0{\cdot}15$	$-1{\cdot}10\pm0{\cdot}14$
Z_{δ_e}/mV_e	$-0{\cdot}47\pm0{\cdot}093$	$-0{\cdot}46\pm0{\cdot}092$	$-0{\cdot}34\pm0{\cdot}091$	$-0{\cdot}43\pm0{\cdot}092$	$-0{\cdot}44\pm0{\cdot}091$
M_α/I_y	$-19{\cdot}78\pm3{\cdot}96$	$-17{\cdot}63\pm1{\cdot}43$	$-17{\cdot}48\pm1{\cdot}16$	$-17{\cdot}72\pm1{\cdot}17$	$-17{\cdot}52\pm1{\cdot}09$
$(M_q + M_{\dot\alpha})/I_y$	$-2{\cdot}38\pm0{\cdot}48$	$-1{\cdot}25\pm0{\cdot}33$	$-0{\cdot}90\pm0{\cdot}31$	$-1{\cdot}14\pm0{\cdot}31$	$-1{\cdot}23\pm0{\cdot}30$
M_{δ_e}/I_y	$-31{\cdot}14\pm6{\cdot}23$*	$-31{\cdot}70\pm3{\cdot}96$	$-25{\cdot}75\pm2{\cdot}94$	$-30{\cdot}51\pm3{\cdot}50$	$-31{\cdot}27\pm3{\cdot}67$
a_1	$0{\cdot}87\pm0{\cdot}17$	—	—	—	$0{\cdot}88\pm0{\cdot}11$
a_2	$0{\cdot}013\pm0{\cdot}003$	—	—	—	$0{\cdot}013\pm0{\cdot}003$
b_1	$0{\cdot}23\pm0{\cdot}046$	—	—	—	$0{\cdot}024\pm0{\cdot}046$
G/τ	100 ± 20	—	—	$89{\cdot}1\pm15{\cdot}0$	—
$1/\tau$	100 ± 20	—	—	$111{\cdot}1\pm17{\cdot}0$	—
$s^2(\alpha)$	—	—	2·78	0·393	0·174
$s^2(q)$	—	0·180	1·14	0·183	0·175
$s^2\left(\frac{gn_z}{V_e}\right)$	—	0·078	0·14	0·078	0·077

* Value used in all tabulated matching. Subsequent examination of available information suggests that −34·24 would be a more firmly based *a priori* value (correctly adjusted for c.g. location). However recalculation of 211–4 shows negligible change.

At this stage no corrections have been applied to measured incidence, α_m. The next case, 211–3, corrects α_m for pitch rate effect, α_s (see Section 3.2) and in addition augments the basic mathematical model (Section 2.1) with the lag equation as described in Section 2.4. This resulted in considerable improvement in the mean square errors, s^2, for all the records, as shown in Table 4, and also produced the much improved angle of incidence match of Figure 4*c*. The lag time constant, τ, was identified as being very small (less than 0·018) and in fact much of the apparent lag of Figure 4*b* was removed by the pitch rate correction, α_s. The improvement in match has been achieved largely as a result of the low identified gain term ($G = 0{\cdot}80$) which would correspond to a calibration slope decrease of 20%. As one might hope, the main identified aerodynamic derivatives have moved closer to the results of case 211–1 which neglected the α_m record in the matching process.

On closer examination of Figure 4*c* it is apparent that the lag model fails to reproduce accurately the initial rise in the measured record. This inadequacy eventually led to the abandonment of the lag model and its replacement by a model which corrects for the dynamic imbalance of the incidence vane as described in Section 2.3. This model was used to match the measured records of α_m (corrected for pitch rate effect, α_s) q_m and n_{z_m} and the results are shown in column 211–4 of Table 4 and in Figure 5. The improved fit for each of the three records is evident. The improvement in the angle of incidence match is the most marked with $s^2(\alpha)$ decreasing from 0·393 for case 211–3 to 0·174. Figure 5 shows an excellent match for all the response variables and in particular the initial portion of the incidence curve is now accurately matched. In addition, the values of the identified aerodynamic derivatives are now very similar to those obtained from case 211–1.

Using these values of the derivatives and the identified values of a_2 and b_1 an estimate can be made for K from the definitions of a_2 and b_1 in Equation 21. This results in values of $K = 0{\cdot}27$ and 0·31 from a_2, b_1 respectively compared with the value of $K = 0{\cdot}30$ used in calculating *a priori* values for a_2 and b_1. However neither a_2 nor b_1 is a strongly determined parameter as is apparent from the small changes obtained in the identified values and Cramer–Rao bounds compared with the *a priori* values and weights. On the other hand, a_1 is a more strongly determined parameter and using a value of $K = 0{\cdot}3$ together with the estimated value for a_1 implies a value for G of 1·01, which suggests that the vane calibration is indeed close to the wind tunnel for this case.

4.2 Non-linear Pitching Moment Curve

The results from flight 210 are summarised in Table 5 with the *a priori* values shown in the first column for reference.

Initially only the q_m and n_{z_m} records were matched using the basic mathematical model of Section 2.1. The results are shown in the column under 210–1 in Table 5 and the matched q record shown in Figure 6*a*. The match is nowhere as good as obtained in the comparable case 211–1 of the previous section. On closer examination of Figure 6*a* it can be seen that while in the early part of the record the measured value of q_m appears to have a phase lead over the calculated q, the reverse applied in the latter part of the record. This systematic phase shift is clearly illustrated in Figure 6*b* which plots the difference between measured and calculated values, or the residuals, against time.

The match can be greatly improved by accounting for the non-linearities in the pitching moment and/or lift curve with incidence as outlined in Section 2.2. With the derivatives M_{α^2}, M_{α^3} and Z_{α^2} added to the model and the pitch rate, q_m, and normal acceleration, n_{z_m}, records again matched, the results are as shown under column 210–2 in Table 5 and a comparison of measured and calculated pitch rate is shown in Figure 7*a*. In calculating the α^2 and α^3 elements of the input vector (Equation 22), the measured angle, α_m, corrected for pitch rate effect, α_s, was used in this case. The improvement achieved by this extended model is quite marked with mean square error $s^2(q)$ decreasing from 0·459 to 0·169 and $s^2(gn_z/V_e)$ decreasing from 0·393 to 0·169. The plot of the residuals in Figure 7*b* also illustrates the improved match. For an ideal match the residual at any one point should be uncorrelated with that of any other point on the record. To check this the autocovariance function for the q-residuals was calculated. This is defined as

$$f(q) = \overline{q(t)q(t+\tau)}/\overline{q^2(t)} \tag{30}$$

TABLE 5
Results from Flight 210

Item	*A Priori*	210–1	210–2	210–3	210–4
Z_α/mV_e	$-0{\cdot}85\pm0{\cdot}17$	$-0{\cdot}73\pm0{\cdot}10$	$-0{\cdot}71\pm0{\cdot}12$	$-0{\cdot}74\pm0{\cdot}10$	$-0{\cdot}74\pm0{\cdot}10$
Z_{δ_e}/mV_e	$-0{\cdot}31\pm0{\cdot}062$	$-0{\cdot}33\pm0{\cdot}061$	$-0{\cdot}32\pm0{\cdot}061$	$-0{\cdot}32\pm0{\cdot}061$	$-0{\cdot}32\pm0{\cdot}061$
M_α/I_y	$-25{\cdot}49\pm5{\cdot}10$	$-18{\cdot}30\pm1{\cdot}12$	$-16{\cdot}17\pm3{\cdot}07$	$-16{\cdot}03\pm2{\cdot}78$	$-16{\cdot}05\pm2{\cdot}97$
$(M_q+M_{\dot\alpha})/I_y$	$-1{\cdot}02\pm0{\cdot}21$	$-1{\cdot}08\pm0{\cdot}18$	$-0{\cdot}99\pm0{\cdot}18$	$-0{\cdot}96\pm0{\cdot}17$	$-0{\cdot}96\pm0{\cdot}17$
M_{δ_e}/I_y	$-35{\cdot}46\pm7{\cdot}09$	$-38{\cdot}13\pm4{\cdot}11$	$-36{\cdot}68\pm4{\cdot}18$	$-36{\cdot}16\pm3{\cdot}97$	$-36{\cdot}51\pm4{\cdot}02$
M_{α^2}/I_y	—	—	$24{\cdot}5\pm191$	$33{\cdot}7\pm146$	$17{\cdot}8\pm87$
M_{α^3}/I_y	—	—	-1597 ± 3880	-1671 ± 3048	-778 ± 1499
Z_{α^2}/mV_e	—	—	$-1{\cdot}13\pm3{\cdot}91$	—	—
a_1	$0{\cdot}93\pm0{\cdot}19$	—	—	$0{\cdot}77\pm0{\cdot}12$	$0{\cdot}74\pm0{\cdot}12$
a_2	$0{\cdot}0091\pm0{\cdot}002$	—	—	$0{\cdot}0090\pm0{\cdot}002$	$0{\cdot}0090\pm0{\cdot}002$
b_1	$0{\cdot}24\pm0{\cdot}048$	—	—	$0{\cdot}25\pm0{\cdot}048$	$0{\cdot}25\pm0{\cdot}048$
b_2	$-0{\cdot}28\pm0{\cdot}056$	—	—	$-0{\cdot}28\pm0{\cdot}056$	$-0{\cdot}28\pm0{\cdot}056$
b_3	$14{\cdot}70\pm2{\cdot}94$	—	—	$14{\cdot}66\pm2{\cdot}94$	$14{\cdot}33\pm2{\cdot}93$
$s^2(\alpha)$	—	—	—	$0{\cdot}466$	$0{\cdot}492$
$s^2(q)$	—	$0{\cdot}459$	$0{\cdot}169$	$0{\cdot}167$	$0{\cdot}184$
$s^2\left(\frac{gn_z}{V_e}\right)$	—	$0{\cdot}393$	$0{\cdot}169$	$0{\cdot}235$	$0{\cdot}249$

where the bars refer to the time average value and τ is a given time shift. The plots of $f(q)$ against τ for the linear and non-linear models are shown in Figure 8 and confirm the improvement achieved using the non-linear model. Although the pitch rate records have been used to illustrate the points made so far, the same conclusions apply to the normal acceleration, n_z, records. It may be noted, finally, in comparing cases 210–1 and 210–2 that although the match has been significantly improved, the estimated values of the aerodynamic derivatives have altered only slightly with the exception, as expected, of M_α/I_y.

The next case, 210–3, matches all three records, α_m, q_m, and n_{z_m}. The non-linear model for the pitching moment curve was retained (i.e. the M_{α^2}, M_{α^3} terms) but a linear model for the Z-force curve was assumed (i.e. the Z_{α^2} term was removed) since the improvement achieved by retaining the Z_{α^2} term was relatively small. The angle of incidence, α_m, was corrected for pitch rate effect, α_s, and the corrected value, $\alpha_m + \alpha_s$ used in calculating the α^2 and α^3 terms of the extended input vector. The complete mathematical model also included corrections for the dynamic imbalance of the incidence vane as described in Section 2.3, which led to the additional parameters a_1, a_2, b_1, b_2 and b_3. The results of case 210–3 are summarised in Table 5 and plots of all relevant variables shown in Figure 9. An excellent match is obtained in all cases. The relatively large mean square error in the incidence match, $s^2(\alpha)$, reflects the higher noise levels on the incidence measurements compared to the other measured quantities (see Figure 9). The slight increase in the value of $s^2(gn_z/V_e)$ compared to case 210–2 can be ascribed to the neglect of Z_{α^2}. The values of the identified parameters are very similar to those from case 210–2. The values of K implied by a_2 and a_3 are 0·30 and 0·32 respectively while the estimated value of a_1 implies a value of $G = 0{\cdot}84$ (for $K = 0{\cdot}30$). This low value of G suggests a substantial change in the incidence vane calibration curve slope for this case ($M = 0{\cdot}96$) in contrast to results in the previous section from flight 211 ($M = 0{\cdot}71$).

The final case, 210–4, is a repeat of 210–3 with the sole difference that instead of using the measured values of incidence ($\alpha_m + \alpha_s$) to calculate the α^2 and α^3 terms of the input vector, these terms were calculated using the values of the state variable α as obtained in 210–3. The results in Table 5 show only minor changes from the results of case 210–3 with the exception of the extracted values of M_{α^2} and M_{α^3}.

The significance of the values of M_{α^2} and M_{α^3} can be illustrated by reference to Figure 10, which plots the pitching moment against total incidence, $\alpha_e + \alpha$. The identified pitching moment takes the form

$$M = M(\alpha = \alpha_e) + \Delta M$$

where the incremental moment, ΔM, is (according to Equation 13):

$$\Delta M = M_\alpha \alpha + M_{\alpha^2}\alpha^2 + M_{\alpha^3}\alpha^3$$

and $M(\alpha = \alpha_e)$ is taken from the wind tunnel results[9] of pitching moment *vs.* incidence, adjusted to the correct centre of gravity position. The values of M_{α^2} and M_{α^3} from cases 210–2 and 210–3 produce almost identical curves over the incidence range covered in the pitch up manoeuvre despite the differences in the actual values of M_{α^2} and M_{α^3}. It is clear that a fairly wide range of values of M_{α^2} and M_{α^3} can lead to almost identical curves over the restricted range of interest and this accounts for the large Cramer–Rao bounds obtained for these parameters. The curve corresponding to case 210–4 is also shown in Figure 10 and differs slightly from the other calculated curve towards the extremes of the α-range. For comparison, the equivalent wind tunnel data[9] at $M = 0{\cdot}95$, is also plotted on Figure 10 and appears to agree very well with the identified results. This is strong support for the approach used and confirms that non-linear aerodynamics can be accommodated successfully within the framework of a linear mathematical model.

4.3 General Discussion

In the present calculations the Cramer–Rao bounds are not strictly correct since they are based on the prescribed D_1 and D_2 matrices rather than the covariance matrices as required by maximum likelihood theory (see References 5 and 6). Nevertheless the relative magnitudes of the calculated bounds are an indication of the amount of confidence to be placed in the identified results. This is particularly true when the *a priori* feature is used. In that case, if the bounds do not differ from the *a priori* weights prescribed, it is an indication that little additional information is contained in the data and the *a priori* value should be accepted for that particular parameter.

Hence, looking at the final results of Flight 211 (case 211–4) and 210 (cases 210–3 and 210–4) in Tables 4 and 5, it is apparent that Z_{δ_e} is a weakly identified derivative and the *a priori* value should not be modified on the basis of the test information available. On the other hand, reasonable confidence can be placed in the identified values of the other four derivatives, Z_α/mV_e, M_α/I_y, $(M_q + M_{\dot{\alpha}})/I_y$ and M_{δ_e}/I_y.

For flight 211, Z_α/mV_e is in good agreement with the *a priori* value but for flight 210, at $M = 0{\cdot}96$, it is significantly less, being $0{\cdot}74$ compared to $0{\cdot}85$. The rapid flow changes which occur at transonic speeds may be the cause of this difference. The estimated values of M_α/I_y and M_{δ_e}/I_y from flight 211 are both approximately 10% less in magnitude than the *a priori* values (see footnote to Table 4). This sort of difference could easily be accounted for by an error in centre of gravity position since the corrections for shift from the wind tunnel reference position (52%) are quite large in this case. Alternatively, a 10% error in the pitch moment of inertia, I_y, could also account for the difference.

For flight 210 good agreement is obtained with M_{δ_e}/I_y but M_α/I_y appears to be considerably lower than the *a priori* value. However, as discussed in Section 4.2, the slope of the M *vs.* α curve varies considerably at $M = 0{\cdot}96$ and inspection of Figure 10 shows that the slope can alter by a factor of 2 over the range of interest. In fact, Figure 10 indicates a reasonably good agreement between the estimated and wind tunnel pitching moment curves.

Looking now at the damping derivative, $(M_q + M_{\dot{\alpha}})/I_y$, the estimated value at $M = 0{\cdot}71$ (flight 211) is little more than half the *a priori* value while at $M = 0{\cdot}96$ (flight 210) it is in good agreement with the *a priori* value. The low value at $M = 0{\cdot}71$ cannot be easily explained away in view of the relatively good agreement of the other moment derivatives and the conclusion is that the *a priori* value is too high and the lower value should be used in any future mathematical model. The Datcom estimate[11] gives a value of $0{\cdot}94$ for $(M_q + M_{\dot{\alpha}})/I_y$ at $M = 0{\cdot}7$ with the c.g. at the $49{\cdot}1\%$ position. This is almost 25% below the present estimated value. Further the value for M_q/I_y of about $0{\cdot}68$ quoted for the Mirage III in Reference 12 is also in line with the Datcom estimates. These values confirm the conclusion that the *a priori* value used in the present case at $M = 0{\cdot}71$ is too high. On the other hand the good agreement at $M = 0{\cdot}96$ suggests that the shape of the damping curve as Mach number changes is different to what had previously been assumed. Further work is planned to establish the variation of damping over the range of Mach numbers from $0{\cdot}7$ to $1{\cdot}2$.

Some comment should be made on the choice of records for the matching process. It has been possible to achieve excellent matches for all the available records, i.e. α_m, q_m and n_{z_m} provided the incidence vane errors were properly accounted for. It has also been shown that successful identification can be achieved using q_m and n_{z_m} records only. For example, comparison of 211–1 with 211–4 or 210–2 with 210–4 show close agreement in the values of the estimated aerodynamic derivatives and equally good matches of the respective time response records. Thus if doubt exists about the accuracy of a particular record, exclusion of that record can still lead to good results. If however, an attempt is made to match an erroneous record e.g. uncorrected incidence measurements, then an all round deterioration in results can occur. For example, compare case 211–1 with 211–2. Similarly, an inferior result is obtained if non-linearities in the M *vs.* α curve are not modelled e.g. compare case 210–1 with 210–2.

5. CONCLUDING REMARKS

A modified Newton–Raphson parameter estimation procedure has been applied to flight data from a 60° delta wing aircraft. The response of the aircraft over a period of 5 seconds ($\omega_n T = 21$) to an elevon pulse input at two Mach numbers, $0{\cdot}71$ and $0{\cdot}96$, was successfully analysed to obtain all the relevant longitudinal aerodynamic parameters. The sampling rate of 60 per second ($\omega_n \Delta t = 0{\cdot}07$) was found to be ample and no problems of numerical convergence were encountered. Records of elevator input and the response variables of incidence, pitch rate and normal acceleration were used in the analysis. Good results were achieved when only pitch rate and normal acceleration were matched and this was confirmed by matching all three variables simultaneously.

In order to match the incidence measurements satisfactorily it was found necessary to correct for pitch rate induced error on the incidence vane and, in addition, to make allowance for inertial contributions to the vane readings, which were not dynamically balanced, and for

possible wind tunnel calibration errors. The vane calibration factor which produces the best match is one of the parameters obtained from the program output and this can then be checked against the wind tunnel calibration.

A technique for including non-linear aerodynamic characteristics within the context of a linear model has been demonstrated. The approach used produced a pitching moment curve in good agreement with wind tunnel test results. Making allowance for the non-linearity of the pitching moment curve also achieved significant improvement in the matching of the pitch rate record at $M = 0{\cdot}96$. The present method of analysis could, with possible advantage, also be applied to extraction of data from wind tunnel tests with oscillating models.

The estimated values of the longitudinal derivatives obtained in the present study seem to be in reasonable agreement with wind tunnel values. One exception appears to be damping in pitch where the results disagree with the *a priori* value at $M = 0{\cdot}71$ but are in good agreement at $M = 0{\cdot}96$. This important area is being studied further with the aim of establishing the variation of the pitch damping over the Mach number range from $0{\cdot}7$ to $1{\cdot}2$.

An important aim of the work reported here has been to test the application of systems identification procedures to available longitudinal flight data. The results have demonstrated a variety of ways in which the program can be used, not only to validate mathematical models and check flight results against data obtained from wind tunnels, but also to obtain information not easily available through other means.

NOTATION

a_1, a_2	Coefficients in Equation 21
A	Matrix of stability parameters, Equation 2
b_1, b_2, b_3	Coefficients in Equation 21
$\mathbf{b}$	Measurement bias vector
b_o	Equation error bias term, Equation 23
B	Matrix of control parameters, Equation 2
$\mathbf{c}$	Unknown parameter vector
$\mathbf{c}_o$	Vector of *a priori* parameter values
$\bar{c}$	Mean aerodynamic chord
C_m	Non-dimensional moment coefficient, $M/1/2\ \rho\ V^2 S\bar{c}$
D_1	Weighting matrix for response variables, Equation 1
D_2	Weighting matrix for parameter estimates, Equation 1
F	Matrix of stability parameters, Equation 3
g	Gravitational acceleration
G	Matrix of control parameters, Equation 3 or gain of vane, Equation 17
h	Height above sea level, m
I_y	Moment of inertia in pitch, kg-m^2
J	Cost functional (Fit error)
K	Constant of proportionality, Equation 18
m	mass, kg
M	Mach number or pitching moment
M_o	Equation error bias term, Equation 10
M_q	Pitching moment derivative w.r.t. q
M_u	Pitching moment derivative w.r.t. u
M_α	Pitching moment derivative w.r.t. α
M_{α^2}	Pitching moment derivative w.r.t. α^2
M_{α^3}	Pitching moment derivative w.r.t. α^3
$M_{\dot{\alpha}}$	Pitching moment derivative w.r.t. $\dot{\alpha}$
M_{δ_e}	Pitching moment derivative w.r.t. δ_e
$\mathbf{n}$	Measurement noise vector
n_z	Normal acceleration in g units
N	Number of data samples
p	Roll rate, rad/s
q	Pitch rate, rad/s
r	Yaw rate, rad/s
s^2	Mean square weighted error
S	Reference wing area, m^2
$\mathbf{t}$	Time, sec
T	Length of measured responses, sec
$\mathbf{u}$	Vector of control input variables
u	Velocity increment in x-direction, m/s
V	Resultant airspeed, m/s
w	Velocity increment in z-direction, m/s
$\mathbf{x}$	Vector of state variables
x	Body axis co-ordinate in forward direction
X	Force in x-direction, N
X_u	X-force derivative w.r.t. u
X_α	X-force derivative w.r.t. α

X_{δ_e}	X-force derivative w.r.t. δ_e
$\mathbf{y}$	Calculated response vector, Equation 3
y	Body axis co-ordinate in lateral direction
$\mathbf{z}$	Measured response vector, Equation 4
z	Body axis co-ordinate in down direction
Z	Force in z-direction, N
Z_o	Equation error bias term, Equation 10
Z_u	Z-force derivative w.r.t. u
Z_q	Z-force derivative w.r.t. q
Z_α	Z-force derivative w.r.t. α
Z_{α^2}	Z-force derivative w.r.t. α^2
Z_{α^3}	Z-force derivative w.r.t. α^3
Z_{δ_e}	Z-force derivative w.r.t. δ_e
α	Angle of incidence increment, rad
α_s	Pitch rate correction, Equation 16
α_d	Inertial correction to α, Equation 18
Δ	Increment
δ_e	Elevator angle increment, positive t.e. down, rad
θ	Pitch attitude increment, rad
ρ	Air density, kg/m^3
σ	Standard deviation
σ_{CR}	Cramer–Rao bound
τ	Time constant, Equation 25, or Time shift, Equation 30
ω_n	Natural undamped frequency, rad/s

Subscripts

a	Normal accelerometer
e	Trim or Equilibrium state
i	Time index
m	Measured value
v	Incidence vane

REFERENCES

1. Burton, R. A., and Bischoff, D. E., More Effective Aircraft Stability and Control Flight Testing Through Use of System Identification Technology. AIAA Paper 76–894, Presented at AIAA Aircraft Systems and Technology Meeting, Dallas, Texas/Sept. 27–29, 1976.
2. Ross, A. Jean, Flying Aeroplanes in Buffet. The Aeronautical Journal, Vol. 81, No. 802, October 1977.
3. Park, G. D. Parameter Identification Technology Used in Determining In-Flight Airload Parameters. Journal of Aircraft, Vol. 14, No. 3, March 1977.
4. Klein, V. Parameter Identification Applied to Aircraft. Cranfield Report Aero. No. 26.
5. Iliff, K. W., and Taylor, L. W. Jr., Determination of Stability Derivatives From Flight Data Using a Newton–Raphson Minimisation Technique. NASA TN D-6579, March 1972.
6. Taylor, L. W. Jr., and Iliff, K. W., Systems Identification Using a Modified Newton–Raphson Method—A Fortran Program. NASA TN D-6734, May 1972.
7. Feik, R. A., Aircraft Mathematical Model Validation—Comments on the Use of a Systems Identification Procedure. ARL/Aero Note 365, August 1976.
8. Wolowicz, C. H., Considerations in the Determination of Stability and Control Derivatives and Dynamic Characteristics from Flight Data. AGARD Report 549, Part 1, 1966.
9. Pollock, N., and Forsyth, G. Wind Tunnel Measurements of the Longitudinal and Lateral Characteristics of a Mirage IIIO Model at Subsonic, Transonic and Supersonic Speeds. ARL/Aero Note 319, January 1970.
10. Forsyth, G. F., Transonic Wind Tunnel Tests of a Duel System (Vanes, Pressure Taps) Gust Probe and a Pitot-Static Probe Mounted Side by Side. ARL/Aero Note 334, January 1972.
11. Hoak, D. E. *et al.*, USAF Stability and Control Datcom. AFFDL, Oct. 1960. Revised to June 1977.
12. Wanner, J. C., Dynamique Du Vol et Pilotage Des Avion. ONERA Publication No. 1976-6.

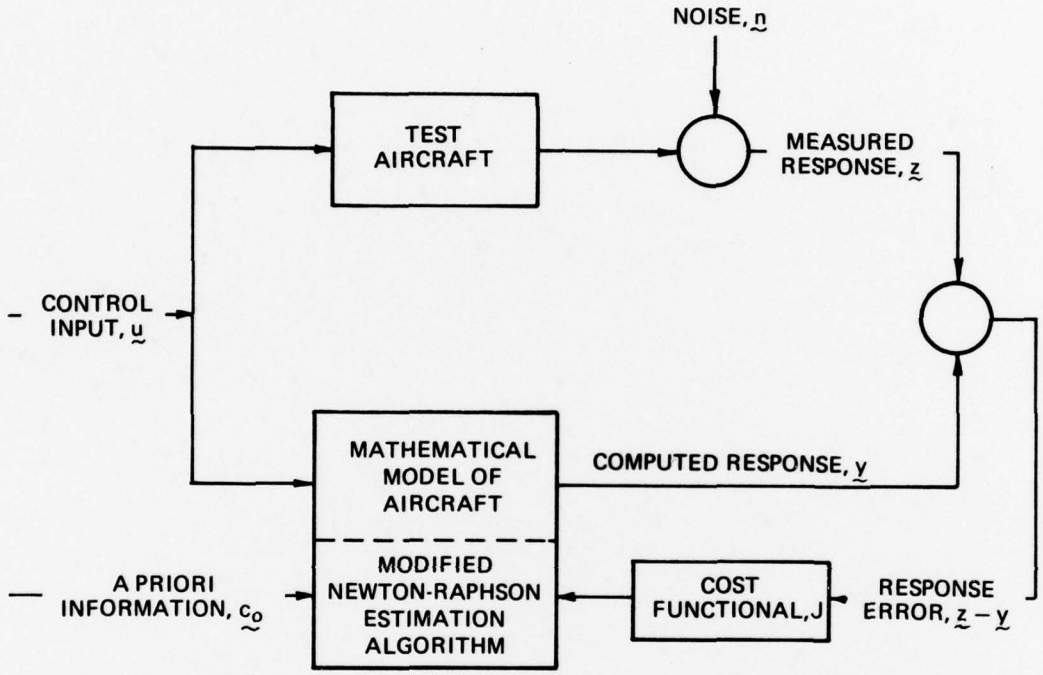

FIG. 1 BASIC CONCEPT OF ESTIMATION METHOD

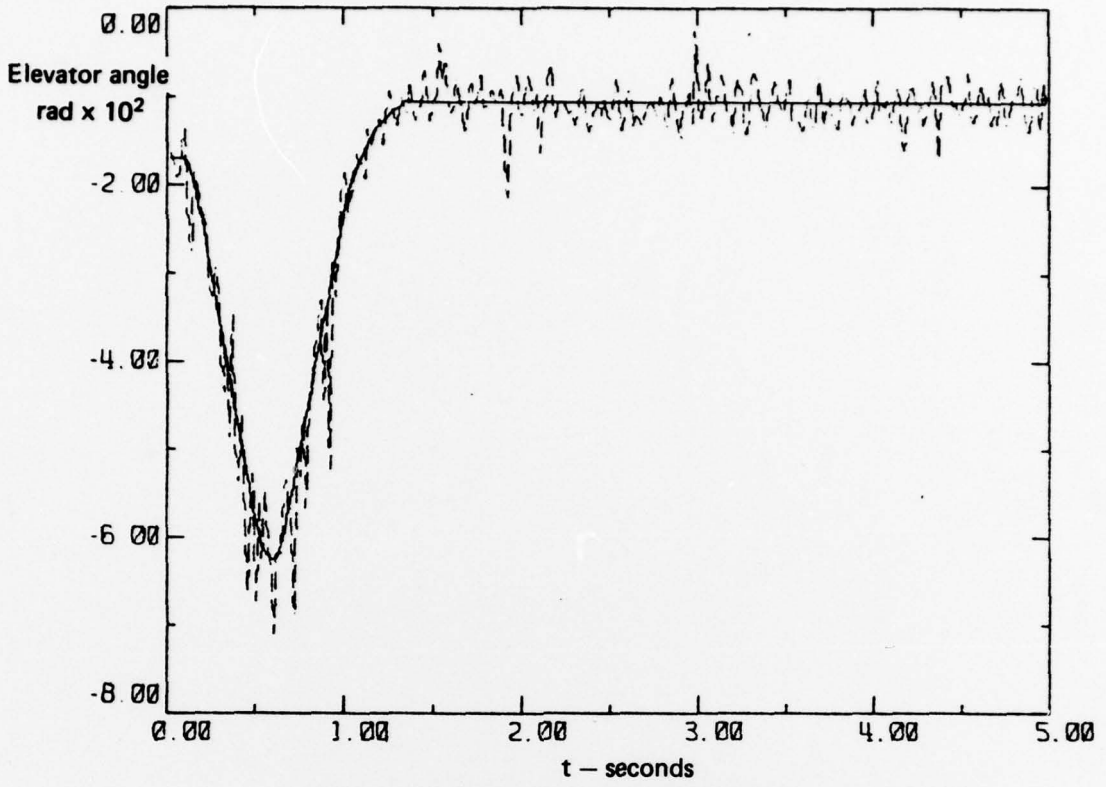

FIG. 2 SMOOTHED ELEVATOR INPUT – FLIGHT 211

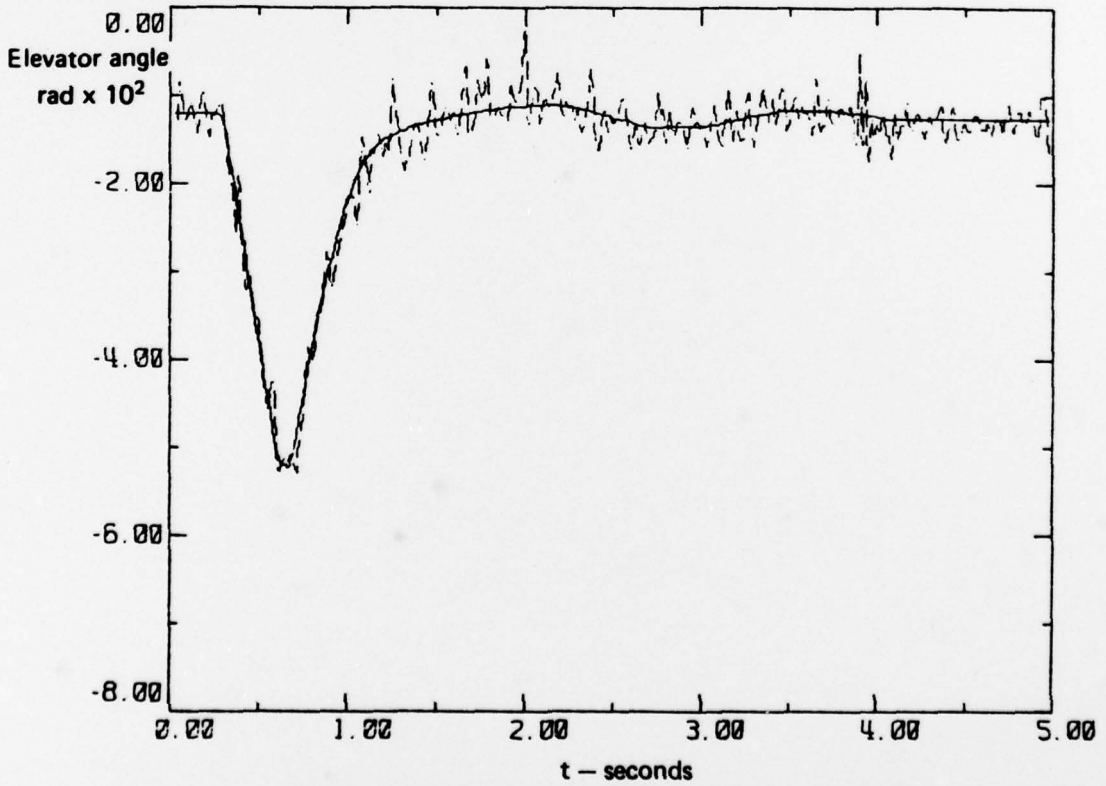

FIG 3 SMOOTHED ELEVATOR INPUT – FLIGHT 210

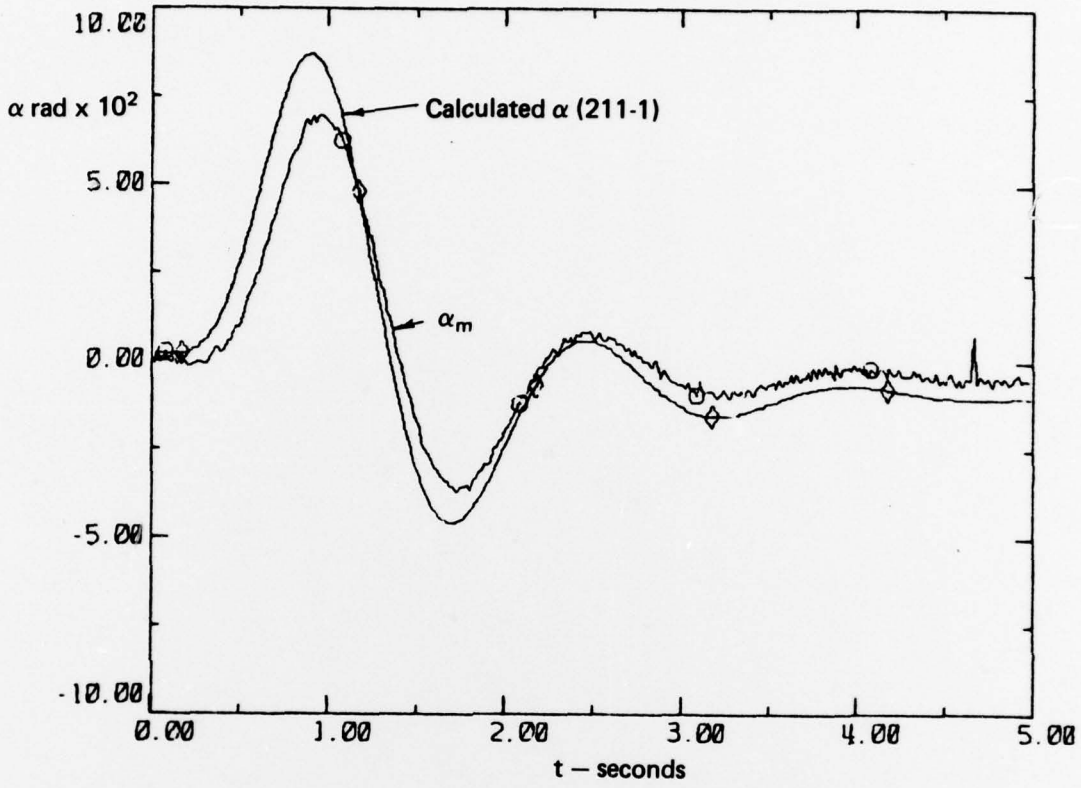

(a) Basic model and measured incidence (unmatched)

FIG. 4 COMPARISON OF ANGLE OF ATTACK FOR FLIGHT 211, M = 0.71

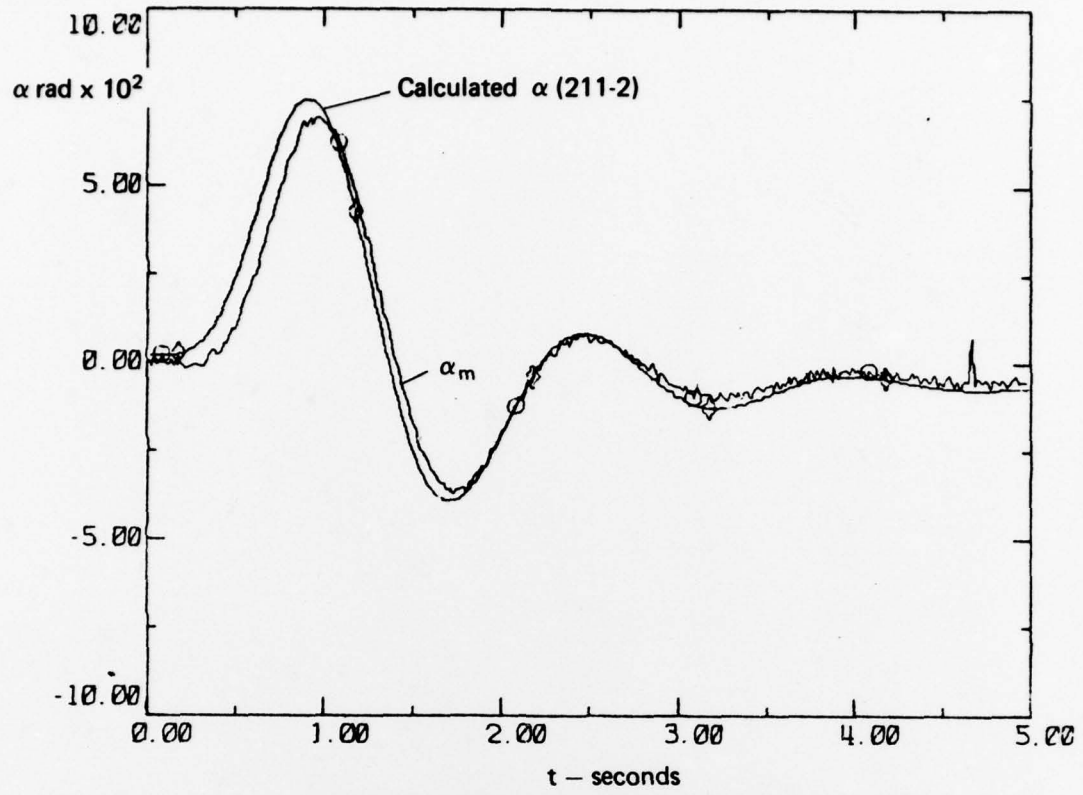

(b) Basic model and measured incidence (matched)

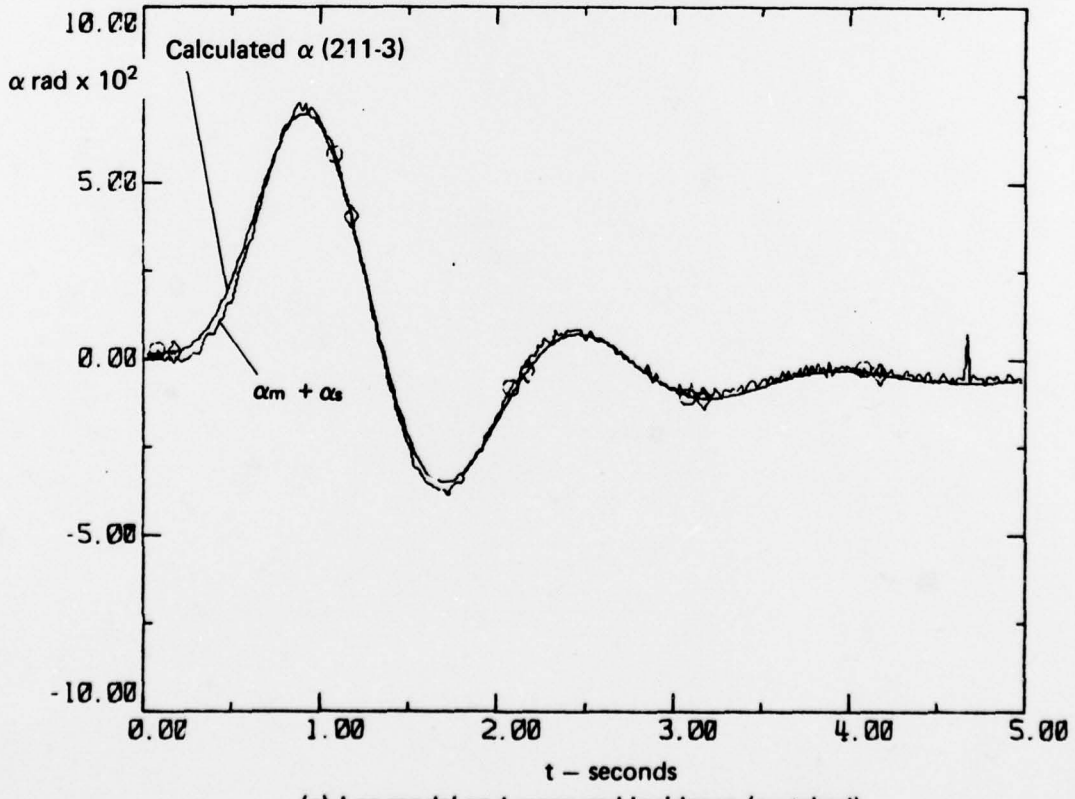

(c) Lag model and measured incidence (matched)

Fig. 4 continued

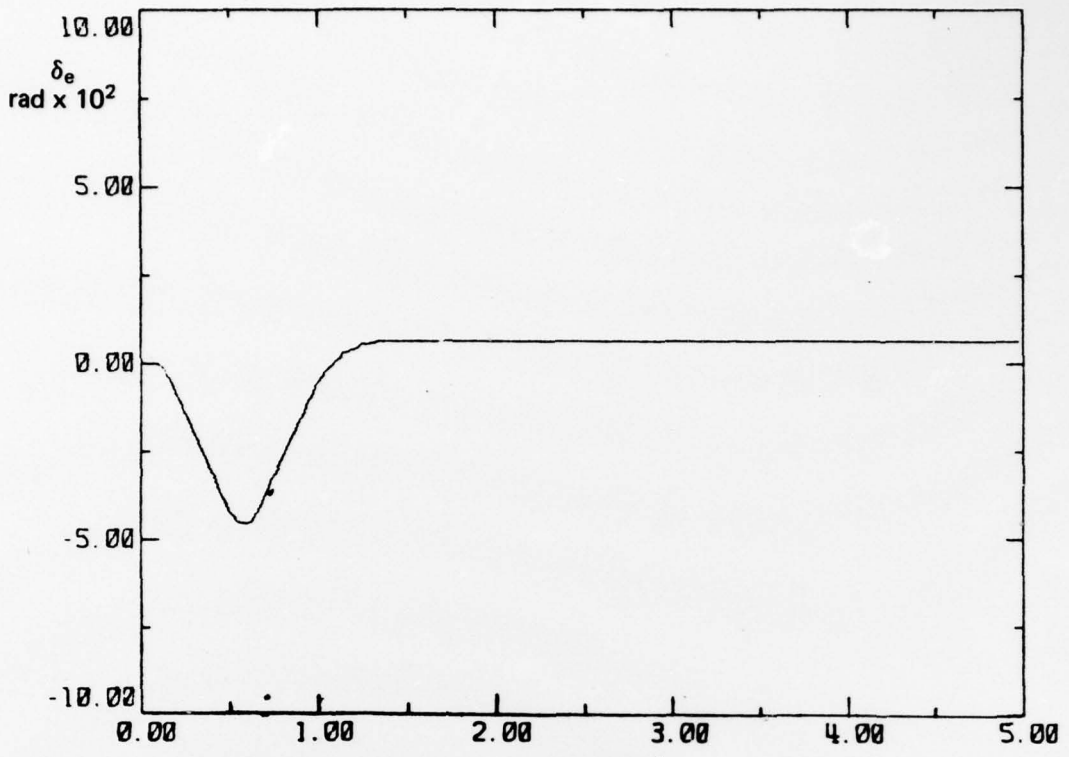

(a) Elevator angle

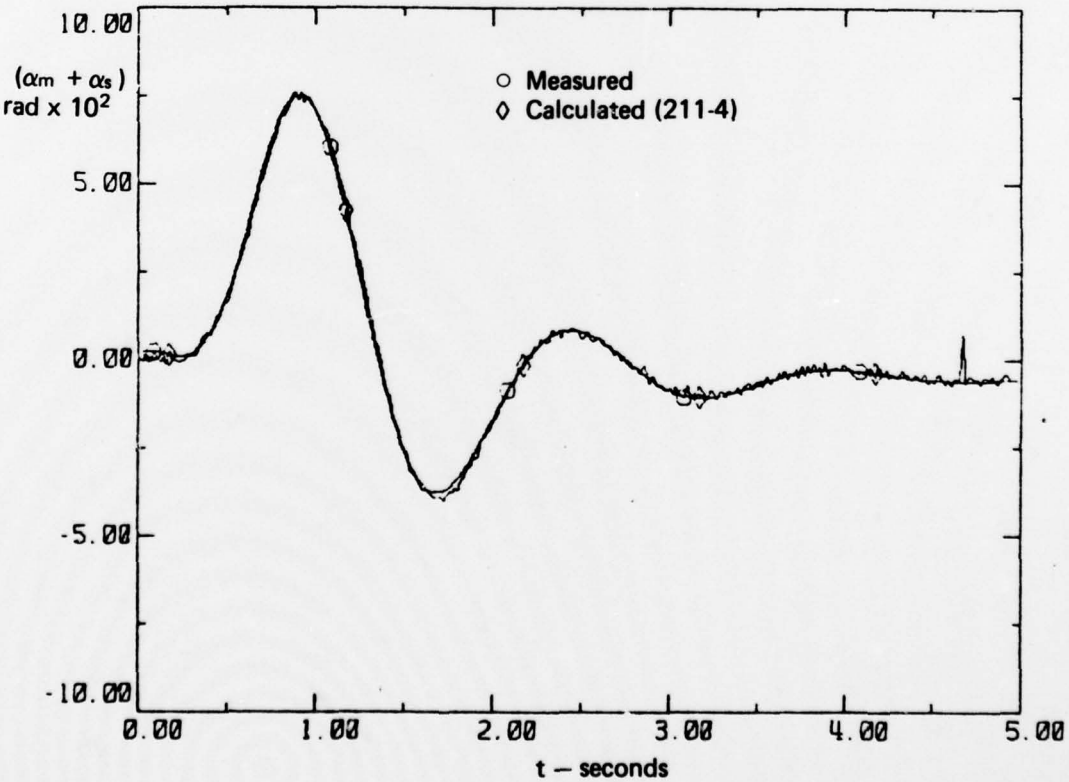

(b) Corrected angle of attack

FIG. 5 FINAL MATCHED RESULTS FOR FLIGHT 211, M = 0.71

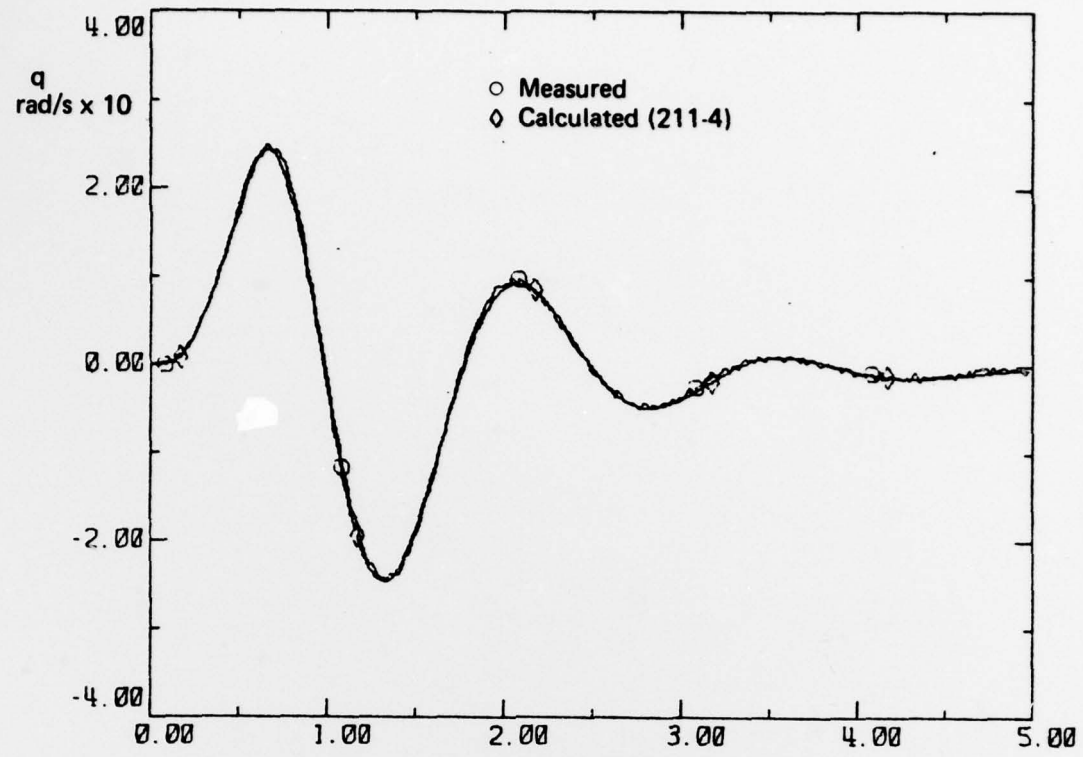

(c) Pitch rate

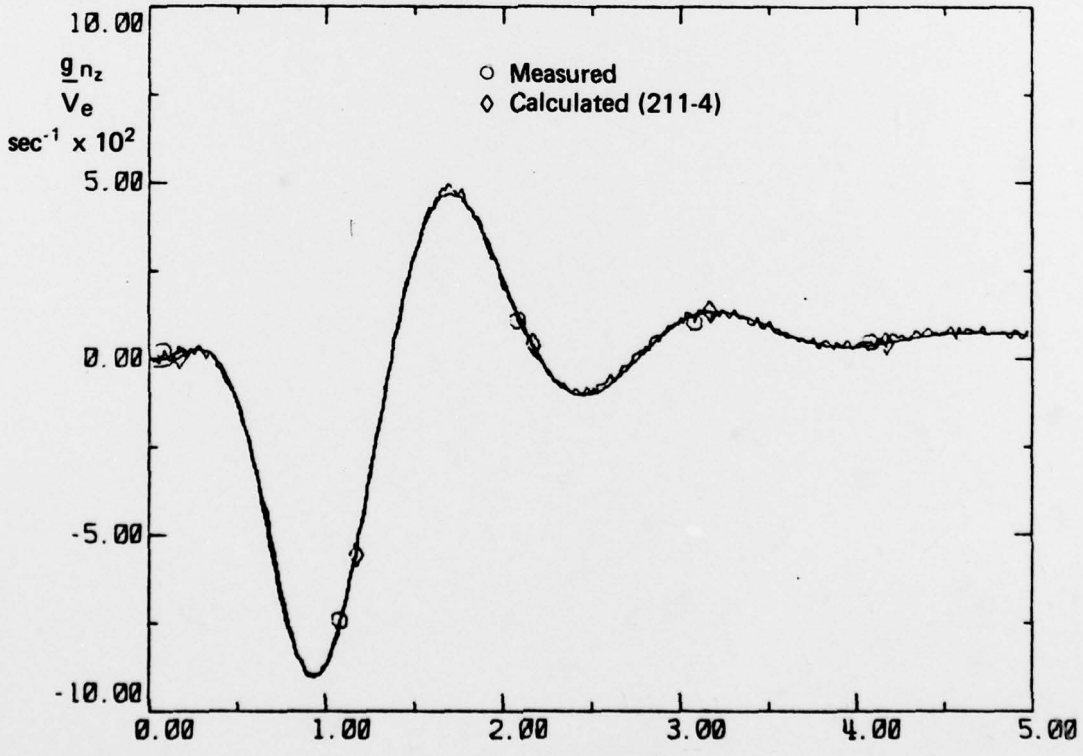

(d) Normal acceleration

Fig. 5 continued

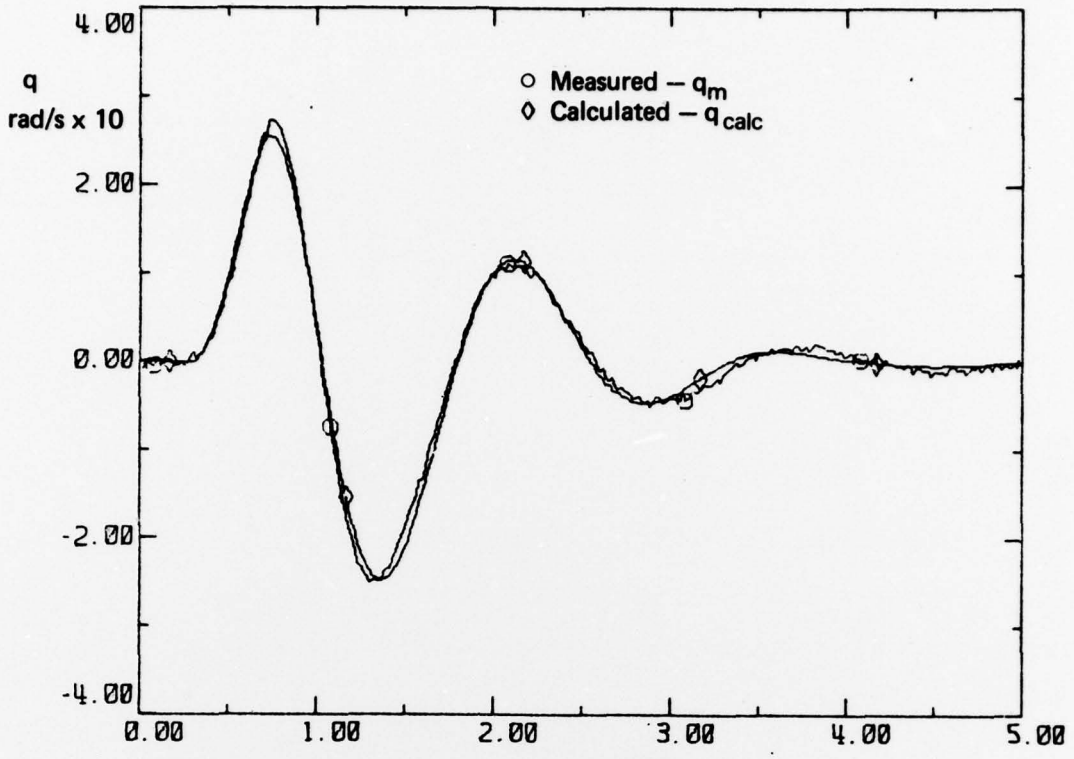

(a) Actual values

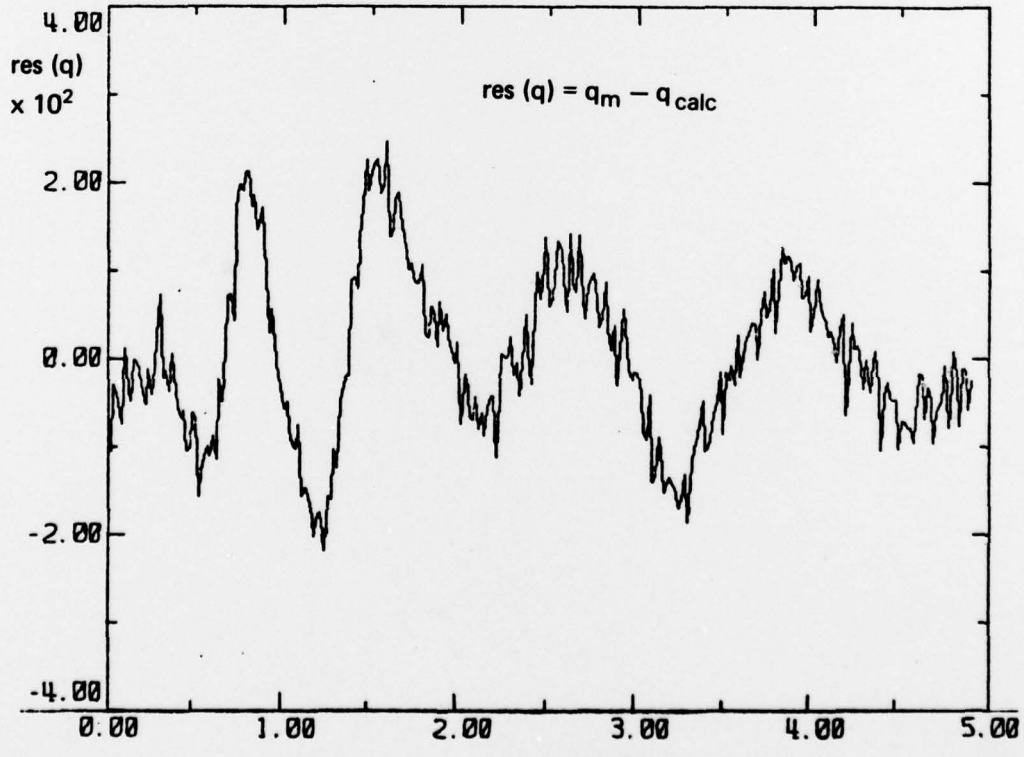

(b) Residues (difference of values in (a) above on expanded scale)

FIG. 6 COMPARISON OF PITCH RATE FOR FLIGHT 210, M = 0.96, LINEAR MODEL

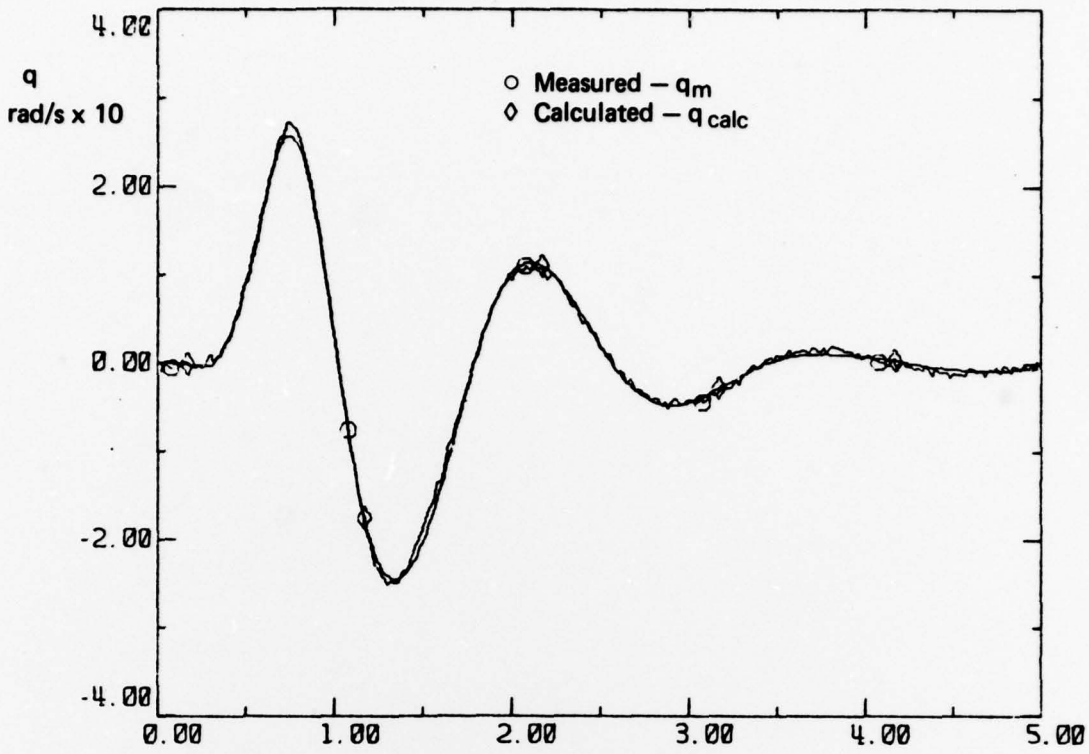

(a) Actual values

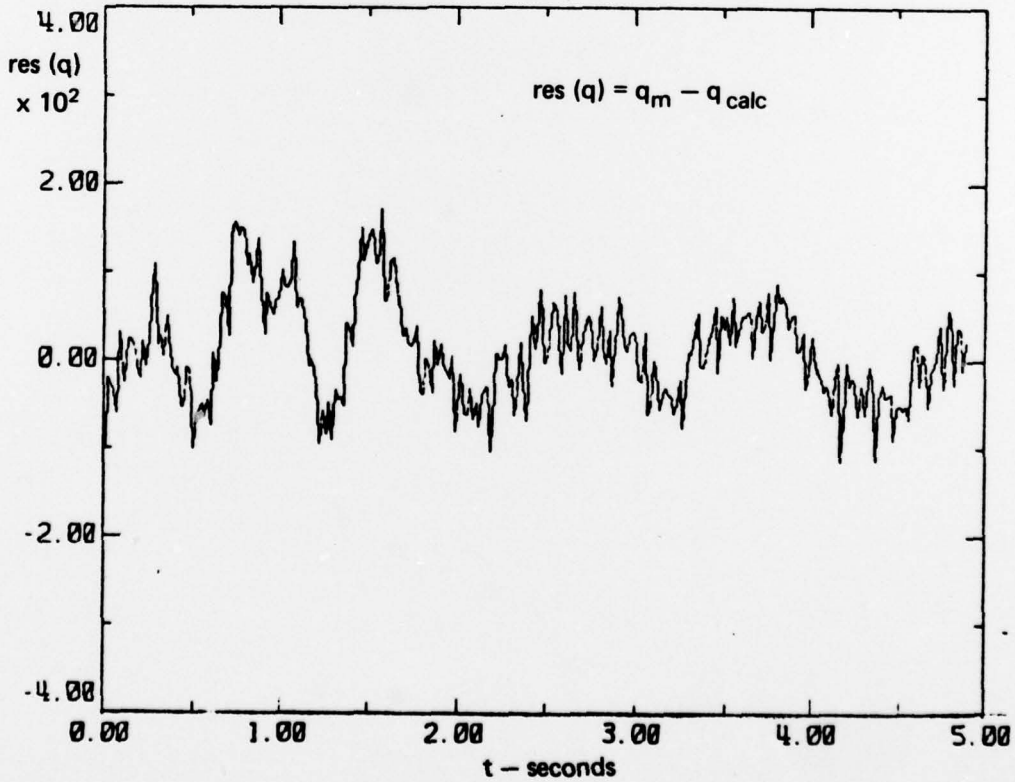

(b) Residues (difference of values in (a) above on expanded scale)

FIG. 7 COMPARISON OF PITCH RATE FOR FLIGHT 210, M = 0.96, NON-LINEAR MODEL

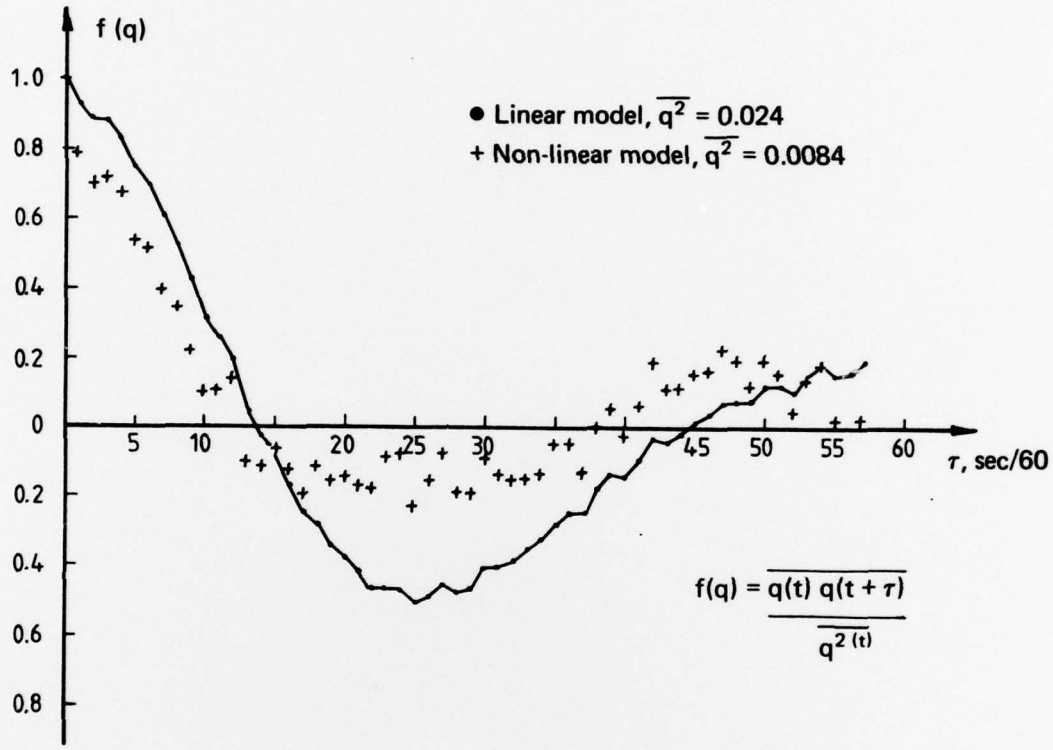

FIG. 8 AUTOCOVARIANCE FUNCTION FOR q – RESIDUALS

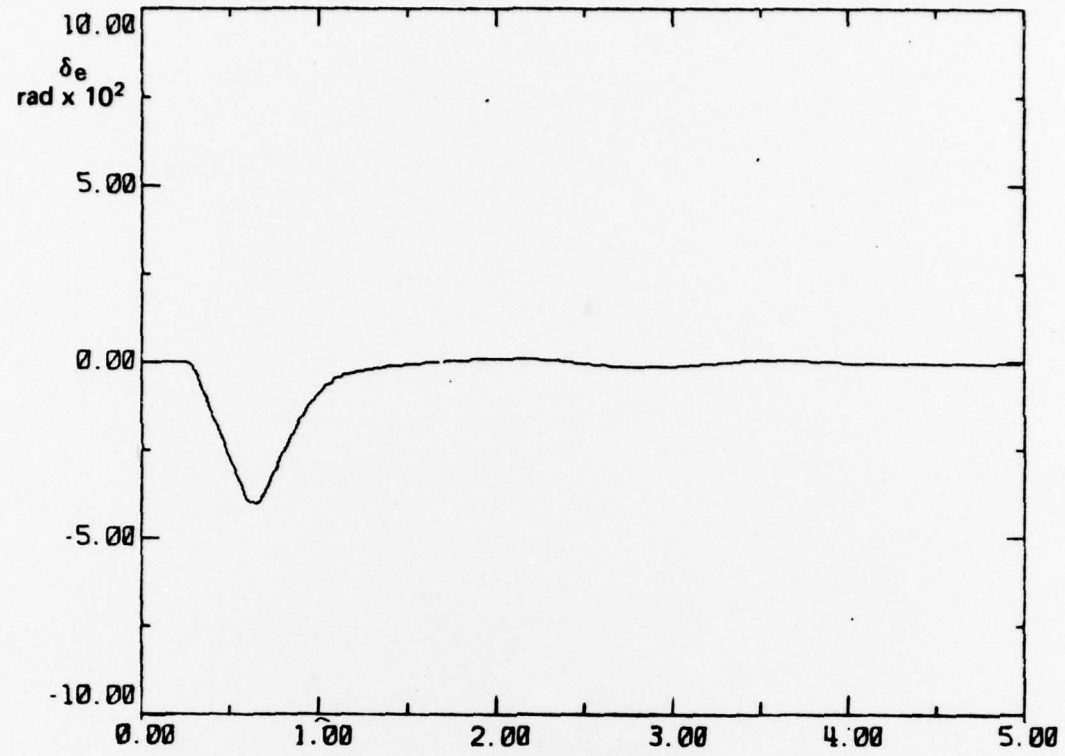

(a) Elevator angle

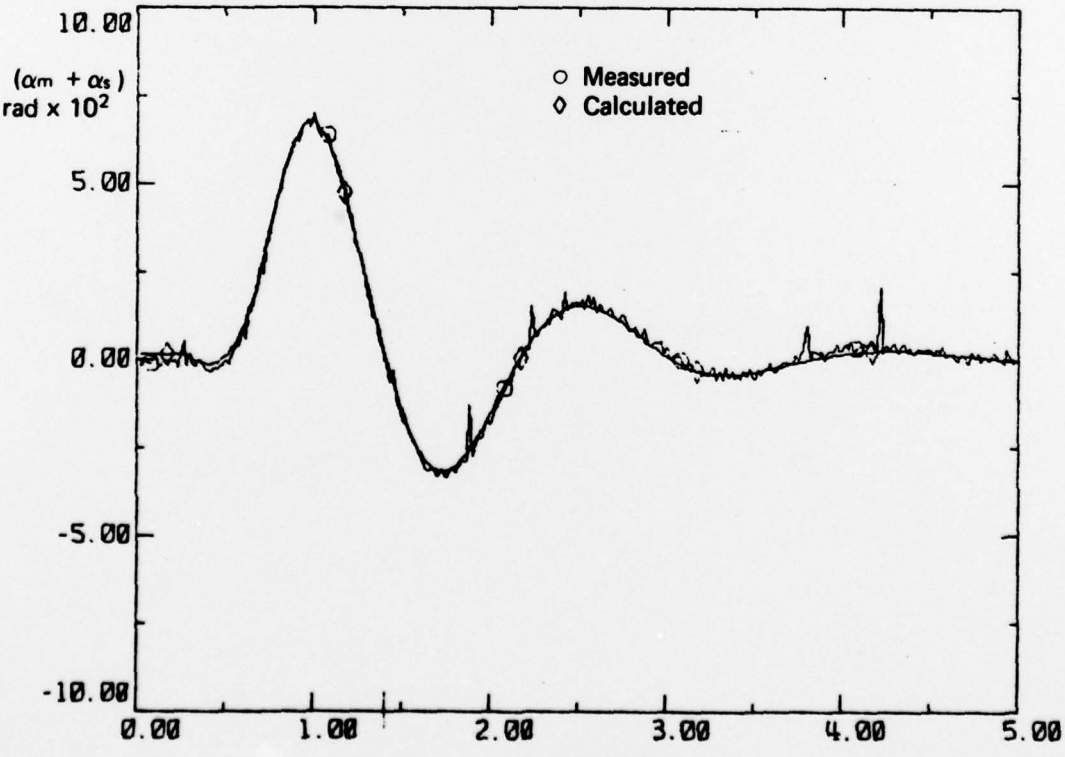

(b) Corrected angle of attack

FIG. 9 FINAL MATCHED RESULTS FOR FLIGHT 210, M = 0.96

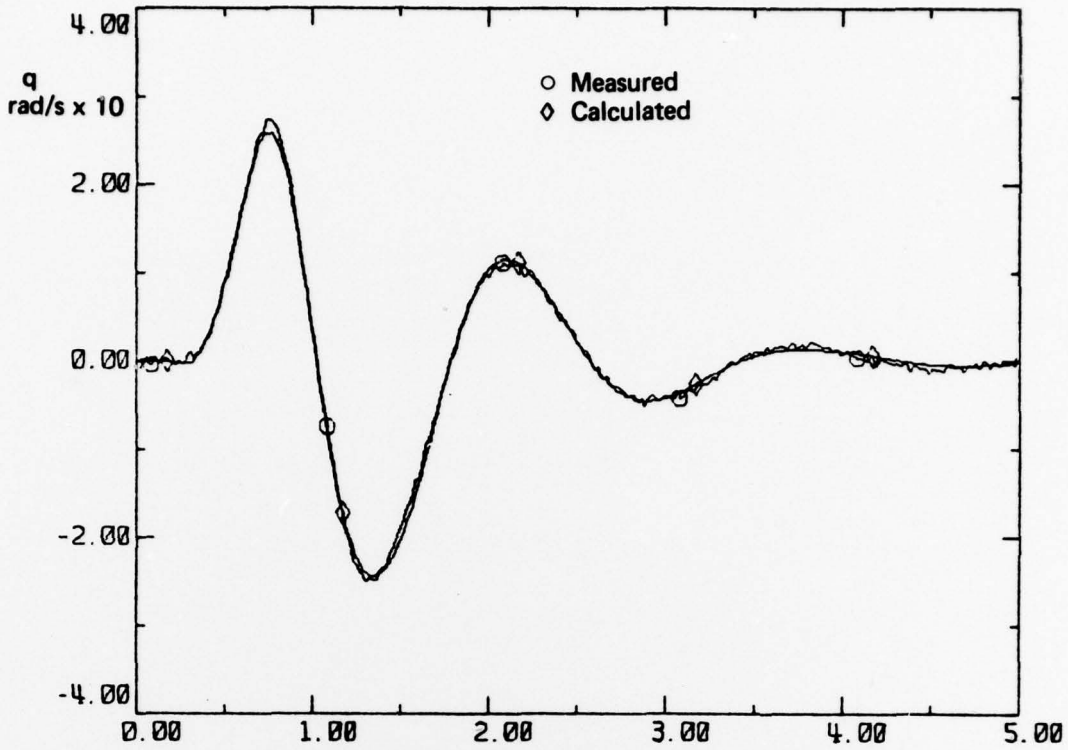

(c) Pitch rate

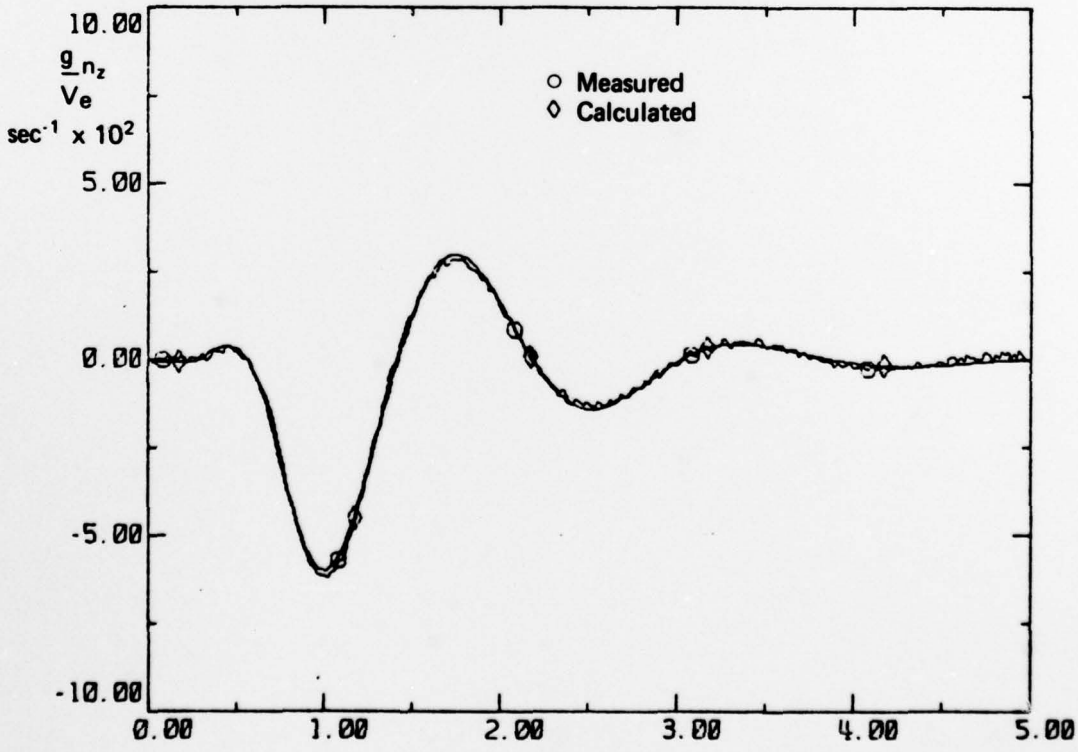

(d) Normal acceleration

Fig. 9 continued

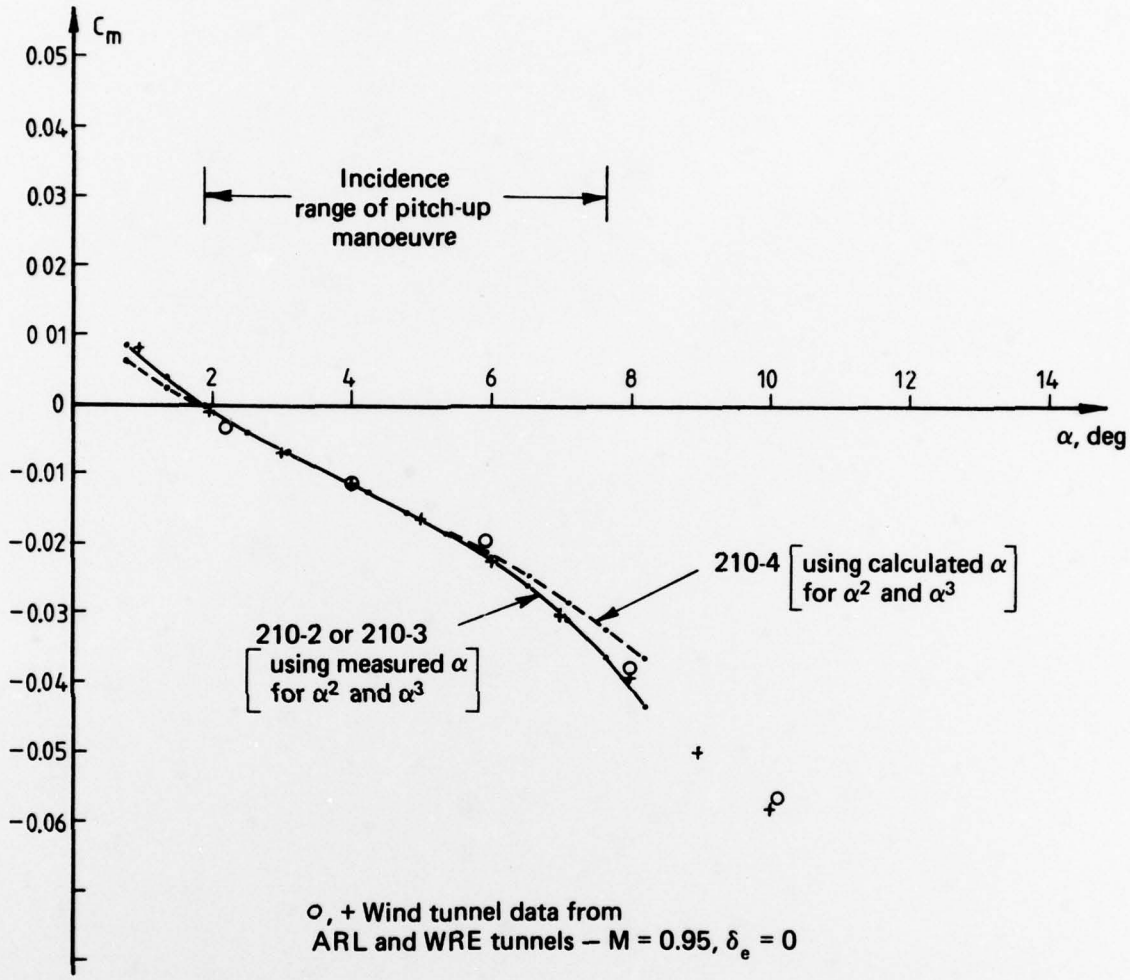

FIG. 10 COMPARISON OF WIND TUNNEL AND IDENTIFIED C_m Vs α CURVES

DOCUMENT CONTROL DATA SHEET

Security classification of this page: Unclassified

1. Document Numbers
   (a) AR Number: AR-001-308
   (b) Document Series and Number: Aerodynamics Note 379
   (c) Report Number ARL-Aero-Note-379

2. Security Classification
   (a) Complete document: Unclassified
   (b) Title in isolation: Unclassified
   (c) Summary in isolation: Unclassified

3. Title: LONGITUDINAL AERODYNAMICS EXTRACTED FROM FLIGHT TESTS USING A PARAMETER ESTIMATION METHOD

4. Personal Author(s): R. A. Feik

5. Document Date: October, 1978

6. Type of Report and Period Covered

7. Corporate Author(s): Aeronautical Research Laboratories

8. Reference Numbers
   (a) Task: DST 74/21
   (b) Sponsoring Agency:

9. Cost Code: 54 7730

10. Imprint: Aeronautical Research Laboratories, Melbourne

11. Computer Program(s) (Title(s) and language(s)):

12. Release Limitations (of the document): Approved for public release

12-0. Overseas:	No.	×	P.R.	1	A		B		C		D		E	

13. Announcement Limitations (of the information on this page): No limitation

14. Descriptors:
Flight tests
Flight simulation
Flight characteristics
Pitching
Damping
Mathematical models
Newton-Raphson method
F111 (Aircraft)
Mirage (Aircraft)

15. Cosati Codes: 0103, 1201, 1402

16.

ABSTRACT

Flight data from a 60° delta wing aircraft have been analysed using a modified Newton-Raphson parameter estimation procedure. The model equations used for the analysis were extended to account for incidence vane errors and non-linearities in the pitching moment curves. Longitudinal derivatives extracted from the data have been compared with wind tunnel measurements and some theoretical estimates and areas of agreement and disagreement identified. The results demonstrate the usefulness of the parameter identification method not only for the validation of aircraft mathematical models and for checking flight results against wind tunnel data but also for obtaining aerodynamic data not easily available through other means.

DISTRIBUTION

Copy No.

AUSTRALIA

DEPARTMENT OF DEFENCE

Central Office

Chief Defence Scientist	1
Executive Controller, ADSS	2
Superintendent, Defence Science Administration	3
Australian Defence Scientific and Technical Representative (UK)	4
Counsellor, Defence Science (USA)	5
Defence Library	6
JIO	7
Assistant Secretary, DISB	8–23

Aeronautical Research Laboratories

Chief Superintendent	24
Superintendent—Aerodynamics Division	25
Divisional File—Aerodynamics	26
Author: R. A. Feik	27
D. A. Secomb	28
J. A. Rein	29
P. Gottlieb	30
C. A. Martin	31
A. J. Farrell	32
N. E. Gilbert	33
C. R. Guy	34
D. C. Collis	35
J. B. Willis	36
D. A. H. Bird	37
C. K. Rider	38
D. A. Frith	39
Library	40

Materials Research Laboratories

Library	41

Defence Research Centre

Library	42
R. L. Pope	43

Air Office

Air Force Scientific Adviser	44
Aircraft Research and Development Unit	45
G. Morgan, Aircraft Research and Development Unit	46
Engineering (CAFTS) Library	47
HQ Support Command (SENGSO)	48

DEPARTMENT OF PRODUCTIVITY

Government Aircraft Factories

STATUTORY, STATE AUTHORITIES AND INDUSTRY

UNIVERSITIES AND COLLEGES

UNITED KINGDOM

UNITED STATES OF AMERICA